Studies on Enzymatic Protein Cell-Surface Anchoring Method and Application to Dendritic Cell Immunotherapy

Studies on Enzymatic Protein Cell-Surface Anchoring Method and Application to Dendritic Cell Immunotherapy

January 2018

Urara TOMITA

Studies on Enzymatic Protein Cell-Surface Anchoring Method and Application to Dendritic Cell Immunotherapy

A Dissertation Submitted to
the Graduate School of Life and Environmental Sciences,
the University of Tsukuba
in Partial Fulfillment of the Requirements for
the Degree of Doctor of Philosophy in Biological Science
(Doctoral Program in Bioindustrial Sciences)

Urara TOMITA

Abstracts

Cell-surface display of functional proteins is a powerful and useful tool for regulating and reinforcing cellular functions. In this study, I used a polyethylene glycol (PEG)-lipids consisting of a long PEG chain and a dioleylphosphatidylethanolamine (DOPE), named the biocompatible anchor for the membrane (BAM) to anchor arbitrary IgG onto the surface of apoptotic tumor cells (ATCs) to enhance the phagocytosis by dendritic cells (DCs) ex vivo, which may improve the efficacy of DC immunotherapy.

The DC immunotherapy has become a promising strategy in adoptive cell therapy, particularly in cancer immunotherapy. These days, DCs loaded with ATCs coated with IgG were found to activate effective antitumor immunity. However, the employment of antigen-specific antibodies is expensive and therefore increases the medical cost. BAM-modified molecules can bind to any type of cells without loss of their activities because the oleyl moieties can be inserted into the ubiquitous lipid bilayer membranes in a noncovalent manner. Therefore, I hypothesized that arbitrary IgG can be readily displayed on ATCs by conjugating with BAM, and that phagocytosis of ATCs into DCs can be enhanced through the interaction between the IgG displayed on the surface of the ATCs and the Fc receptor expressed on DCs.

First, I attached BAM to IgG via amine coupling reaction. This simple method was successfully applied to four types of mammalian cells. Furthermore, treatment of ATCs with the IgG-BAM conjugate increased the phagocytosis ratio of ATCs by DCs, however, the effect was only about two-fold compared to no treatment. Since BAM are attached to the random lysine residue of IgG in this method, Fc-Fc receptor interaction might be disturbed by some BAM attached to Fc region. Therefore, I hypothesized that site-specific

lipidation of IgG is the best way to display IgG(Fc) on the cell surface without losing native activities between Fc and Fc receptor.

Consequently, I developed a method for displaying Fc on the surface of ATCs through *in situ* enzymatic site-specific modification of BAM. Site-specific modification of proteins was performed via sortase A (SrtA)-mediated transpeptidation reactions. This enzyme recognizes substrates that contain an LPETG sequence and cleaves the amide bond between T and G, then react with the triglycine moiety of the peptides. I prepared LPETG-fused Fc domains of mouse IgG1 and IgG2a (Fc1-LPETG and Fc2a-LPETG) and GGGYC peptide conjugated BAM via thiol-maleimide chemistry. Fc1 and Fc2a were successfully attached to BAM displayed on ATCs through *in situ* SrtA-mediated modification. In addition, the phagocytosis rate of ATCs by DCs was increased almost four-fold by displaying Fc2a on the surface of ATCs. Furthermore, vaccination of the DCs which phagocytized Fc2a-BAM treated ATCs induced stronger tumor immunity and delayed tumor development in mouse. On the other hand, display of Fc1-LPETG showed only a slight increase in the phagocytosis rate. The difference in the phagocytosis rates between Fc1 and Fc2a is assumed to be derived from the property that IgG2a induce more active immune effector responses than IgG1 by interacting with Fc receptor, which indicates that site-specifically lipidated Fc maintained natural reactivity between Fc receptor.

According to this study, the enzymatic method for displaying Fc on ATCs was successfully shown to induce strong Fc-Fc receptor interaction for effective DC immunotherapy. In addition, this method is applicable to broad cancer because this method could opsonize ATC with arbitrary IgG, without employing the tumor-specific IgG, which is difficult to obtain for any tumor cells and is expensive. Thus, the combined

use of a BAM and SrtA enzyme represents a very effective and simple approach to display target proteins on cells via exogenous incorporation onto cell membranes. This approach will not only lead to objective clinical responses in DC vaccines, but also become a promising tool for regulating and reinforcing cell-cell interactions in cell and tissue engineering fields.

Contents

Abbreviations

ATC	Apoptotic tumor cell
BAM	Biocompatible anchor for membrane
CD	Cluster of differentiation
CFSE	(5 and 6)-Carboxy fluorescein diacetate succinimidyl ester
CLSM	Confocal laser scanning microscopy
CTL	Cytotoxic T-lymphocyte
DC	Dendritic cell
DMSO	Dimethyl sulfoxide
DOPE	1,2-Dioleoyl-sn-glycero-3-phosphoethanolamine
EDTA	Ethylenediaminetetraacetic acid
EGFP	Enhanced green fluorescent protein
FACS	Fluorescence-activated cell sorter
FBS	Fetal bovine serum
Fc	Fragment-crystalline
FcγR	Fc gamma receptor
Fmoc	9-fluorenylmethyl carbamate
RP-HPLC	Reversed-phase high-performance liquid chromatography
HRP	Horseradish peroxidase
IgG	Immunoglobulin G
MA	Maleimide
MALDI-TOF-MS	Matrix-assisted laser desorption ionization time-of-flight mass spectrometry

MOPS	3-(N-morpholino)-propanesulfonic acid
MHC	Major histocompatibility complex
NHS	N-Hydroxysuccinimide
NK	Natural killer cell
PBS	Phosphate-buffered saline
PCR	Polymerase chain reaction
PE	Phycoerythrin
PEG	Polyethylene glycol
Tris	Tris (hydroxymethyl) aminomethan

List of figures

Chapter 1. General introduction

1.1 Cell-surface protein modification

Membrane proteins are key components of biological recognition systems used in cell-cell or cell-extracellular matrix interactions. Hence, cell surface modifications with functional proteins represent a powerful and useful tool for regulating and reinforcing cellular functions in cell engineering and cell therapy [1]. Compared with protein expression through gene transfer, direct protein transduction from the extracellular medium is more rapid, easily controllable in a concentration-dependent manner, and reliable because it does not require unpredictable processes such as transformation, folding and intercellular trafficking [2]. In particular, the incorporation of proteins into the cell membrane does not involve the troublesome transduction across the cellular membrane. Thus, many approaches for protein transduction onto cellular membranes have been studied. The reported methods can be classified broadly into two categories: modification of cell membranes [3, 4] and protein lipidation [5, 6]. In the former case, chemical and metabolic modification of membrane biomolecules is potentially toxic and may perturb cell physiology [7]. Therefore, recently, transduction of artificially lipidated proteins through noncovalent insertion of the lipid into the cell membrane has been reported as an attractive alternative approach. In particular, site-specific lipidation of the protein is the best way to display target proteins on the cell surface without losing native activities.

Polyethylene glycol (PEG)-lipids consisting of a long PEG chain and a dioleylphosphatidylethanolamine (DOPE) were previously reported by Kato et al. as a biocompatible anchor for biomembranes (abbreviated to BAM) (Figure 1-1) [5]. BAM-modified molecules can bind to any type of cell because the oleyl moieties can be inserted

into the ubiquitous lipid bilayer membranes in a noncovalent manner [5]. By attaching to BAM, various biomolecules such as biotin [5], an antagonistic peptide [8] and green fluorescent protein [5] were spontaneously displayed on living cells without loss of their activities. Other groups have also modified cell surfaces with functional biomolecules using PEG-lipids [1, 9, 10].

1.2 Dendritic cell immunotherapy for cancer treatment

The dendritic cell (DC) immunotherapy (Figure 1-2) has become a promising strategy in adoptive cell therapy, particularly in cancer immunotherapy [11, 12]. For DC vaccines against cancer, DCs are loaded with tumor antigens ex vivo, and upon administration into patients, the DCs with presenting antigenic epitopes can activate anti-tumor effector T and B lymphocytes, and are capable of promoting natural killer (NK) T cells or NK cell activation [13]. Subsequently, these activated mediator and effector cells are reported to reject tumors in numerous studies using animal models [14, 15]. However, although a large number of patients had received DC vaccines in clinical trials, only a limited number of objective clinical responses have been reported [11, 14, 15]. This disappointing result has prompted further studies examining each step in DC vaccination, such as source and ex vivo manipulation of DCs, antigen-loading of DCs, timing and dosing of DC administration and the route of DC administration. In particular, the antigen-loading of DCs is critical because the choice of antigen influences the specificity of the immune response, and the choice of adjuvant defines the quality and magnitude of the anti-tumor response [14, 16].

The ideal tumor antigen for a DC vaccine should induce a broad repertoire of anti-

tumor immunocytes with high avidity for tumor cells. However, in current trials, single MHC-class-I-restricted synthetic peptides are the most commonly used therapeutic antigens. The use of such single synthetic peptides is restrictive because it provides a limited repertoire, such as the possible occurrence of promoting tumor antigen escape variants and the limited activation of cytotoxic T-lymphocytes (CTL) [11, 17]. In addition, synthetic peptides-based DC vaccinations require prior knowledge of the sequence of the suitable-antigenic epitopes [16]. Conversely, over a decade ago, whole apoptotic tumor cells (ATCs) were found to represent promising antigen sources, because ATCs contain a broad spectrum of known and unknown antigens [16, 18, 19]. The use of ATCs potentially overcomes the limitations of synthetic peptides-based DC vaccinations. Such an approach has been presented, in which, DCs loaded with ATCs could induce activation of CTLs and helper T cells, as well as NK and γδ T cells [16]. Previous reports have suggested that activation of NK cells by DCs may be required for antitumor immunity in MHC-class-I-negative malignant tumors [20], and under certain conditions for successful CTL activation [21]. Thus, ATCs may provide a useful and effective source of antigens for overcoming the current problems associated with DC vaccine strategies.

Antigen-immunoglobulin G (IgG) complexes can efficiently sensitize immature DCs for activation of both CTLs and helper T cells in DC vaccine-based antitumor immunity [22, 23]. IgG-complexed antigens are internalized into DCs through the uptake mediated by receptors for the Fc domain of IgG (FcγR), and then, the antigenic peptides derived from the antigens are presented on MHC class I as well as MHC class II cells. In addition, the use of IgG can promote antigen presentation 100-fold more efficiently over pinocytosis of soluble antigens and effectively induce DC maturation [22]. These

advantages of antigen-IgG complexes were confirmed in a ATCs-based DC vaccination. Akiyama et al. reported that the ATCs bearing IgG, which were prepared by chemically modifying cell membranes with IgG, provided a more efficient vaccination against tumors [17]. However, chemical modification of the membrane of ATCs may alter the properties of antigens derived from tumor membrane proteins. Instead of chemical modification of IgG, tumor-specific antibodies can be attached onto the surface of tumor cells via their molecular recognition. Still, the employment of antigen-specific antibodies is expensive and therefore increases the medical cost [23, 24]. Consequently, alternative methods of displaying IgG on the ATC surface is likely to be required for the development of inexpensive and effective DC vaccines.

In this study, to prepare an ATC-IgG complex using a simple and inexpensive approach, I used BAM for anchoring IgG onto the surface of ATCs. I hypothesized that arbitrary IgGs can be readily displayed on ATCs by conjugating with BAM, and that phagocytosis of ATCs by DCs can be enhanced through the interaction between the IgG displayed on the surface of the ATCs and the FcγR expressed on DCs.

1.3 Objective of this study

In this study, I developed a simple and inexpensive method for attaching IgG on the cell surface to enhance phagocytosis of ATCs by DCs ex vivo. To anchor arbitrary IgG on the surface of ATCs, I used BAM. In chapter 2, I developed random IgG-BAM conjugate which was successfully modified on to various types of cancer cells. Treatment of ATCs with the random IgG-BAM conjugate increased the phagocytosis ratio of ATCs by DCs two-fold when compared to no treatment. Although this phagocytosis-enhancing

effect was nearly identical to treatment with a tumor-specific IgG, the effect was still limited. To improve the effect of IgG-BAM conjugate, in chapter 3, I developed site-specific IgG(Fc)-BAM conjugate by applying SrtA-mediated *in situ* enzymatic reaction. The phagocytosis rate of ATCs by DCs was increased almost four-fold by displaying site-specific IgG(Fc)-BAM conjugate. Furthermore, vaccination of the DCs which phagocytized site-specific IgG(Fc)-BAM treated ATCs induced stronger tumor immunity and delayed tumor development in mouse. Finally, in general discussion, I describe the possibility of combination use of SrtA and BAM as a useful tool for regulating and reinforcing cell-cell interactions in cell and tissue engineering fields.

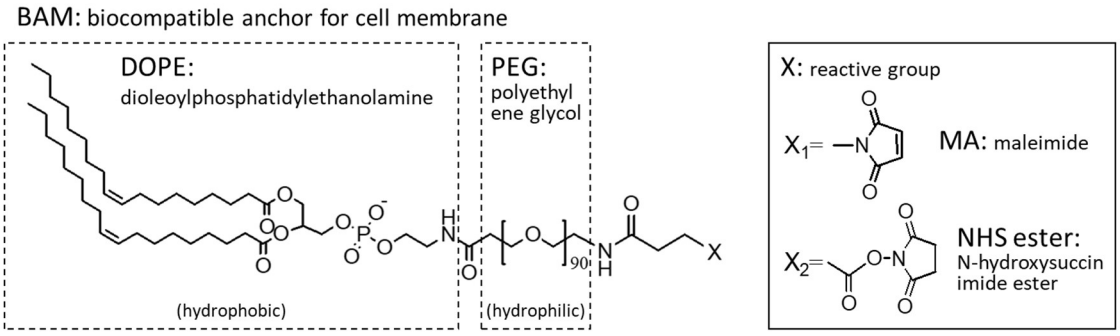

Figure 1-1. Chemical structure of biocompatible anchor for cell membrane (BAM).

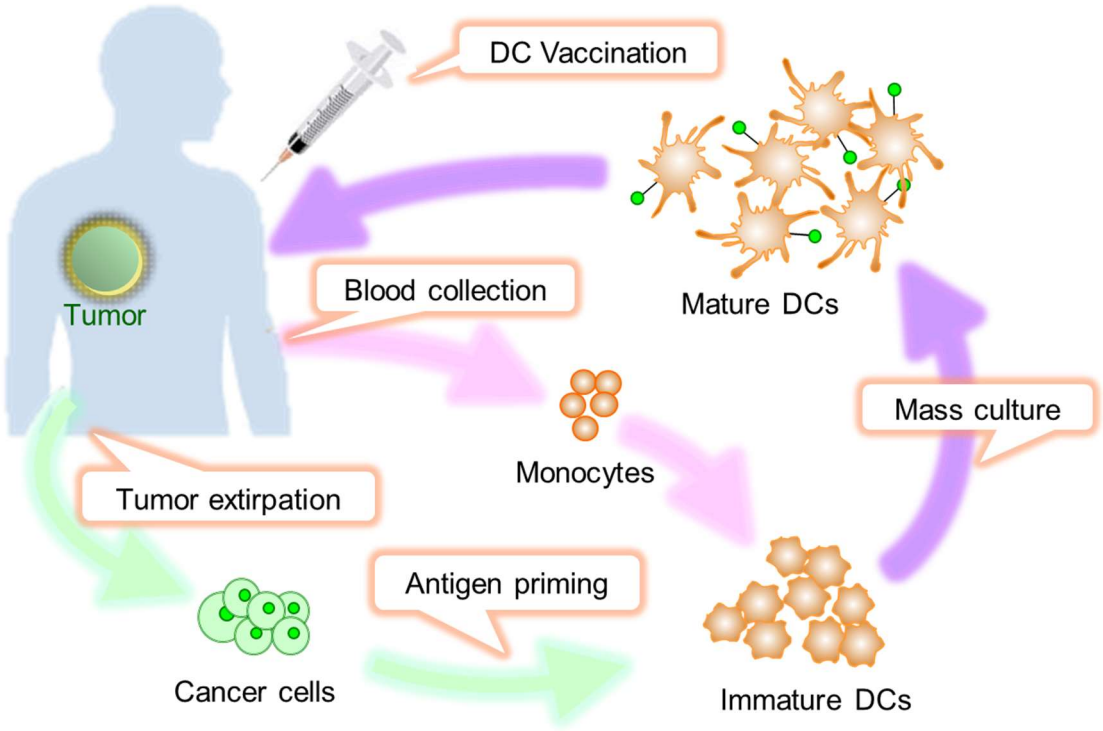

Figure 1-2. The outline of general dendritic cell immunotherapy for cancer treatment.

Chapter 2. Studies on random IgG-BAM conjugate and enhancement of dendritic cell phagocytosis of apoptotic cancer cells

2.1 Introduction

In this study, to develop a simple and inexpensive method for attaching IgG on the cell surface to enhance phagocytosis of ATCs by DCs ex vivo, I used BAM for anchoring IgG onto the surface of ATCs. BAM-modified IgG can bind to any type of cancer cell because the oleyl moieties can be inserted into the ubiquitous lipid bilayer membranes. Therefore, arbitrary IgGs can be readily displayed on ATCs by conjugating with BAM, and that phagocytosis of ATCs into DCs can be enhanced. In this chapter, I used BAM with NHS ester reaction group to conjugate with amine group of IgG (Figure 2-1). Initially, I optimized the conditions of amine coupling reaction between IgG and BAM. The IgG-BAM conjugates prepared under various conditions were tested for their incorporation into cancer cells, and the incorporation rate was investigated using flow cytometry. Then I examined if the IgG-BAM treatment could enhance phagocytosis of ATCs by co-culturing with DCs.

2.2 Materials and methods

2.2.1 Chemicals, antibodies and cell-lines

All chemicals were commercially available and used as supplied without further purification. Purified mouse IgG_{2a} was purchased from Beckman Coulter (CA, USA). Anti-human tumor cell specific antibody (SF-25) was purified from hybridoma-induced mouse ascites by protein A-Sepharose chromatography. For immunostaining of DC, phycoerythrin (PE)-conjugated mouse anti-CD11c antibody (Bioscience, CA, USA) was used. Cy3 or Cy5-labeled anti-mouse Fc antibody (Jackson ImmunoResearch laboratories,

PA, USA) was used for staining Fc. Cell lines, HeLa and Ba/F3 were purchased from ATCC (VA, USA). HepG2, B16 and the hybridoma secreting SF-25 were kindly provided by Tella, Inc (Tokyo, Japan). These cells were cultured in RPMI1640 or DMEM (Nissui, Tokyo, Japan) supplemented with 10% FBS, 2.05 mM l-glutamine, 30 μg/mL kanamycin and 0.2% $NaHCO_3$.

2.2.2 Synthesis of BAM

BAM was synthesized by coupling dioleylphosphatidylethanolamine (DOPE, COATSOME ME-8181 from NOF Corporation, Tokyo, Japan) and PEG disuccinimidylglutarate (SUNBRIGHT DE-050GS from NOF Corporation). DOPE (17.6 mg, 28.8 μmol) and PEG disuccinimidylglutarate (151 mg, 30.2 μmol) were dissolved into 10 mL of anhydrous dichloromethane. Distilled triethylamine (60 μL, 431 μmol) was added, and the mixture was left to stir at room temperature for 1 h. After checking the consumption of DOPE on a thin layer chromatography, the crude product was precipitated by adding into 200 mL of diethyl ether, followed with centrifugation. The supernatant was removed by decantation. Vacuum drying the precipitation yielded white solid (132 mg, 84%).

2.2.3 Preparation of BAM-conjugated IgG

BAM-conjugated IgG (IgG-BAM) was prepared by reacting mouse IgG and BAM in borate buffer (100 mM, pH 8.3) including 2.5% DMSO. The final concentration of IgG was 1 mg/mL (6.67 μM), and that of BAM was varied from 6.60 to 330 μM. The reaction mixture was incubated for 1 h at room temperature and the reaction was quenched by adding Tris-HCl buffer (pH 8.0) to give a final concentration of 50 mM. The product

solution was purified by dialysis against PBS to remove unconjugated BAM, DMSO and a by-product. The purified products were analyzed by sodium dodecyl sulfate-polyacrylamide gel electrophoresis (SDS-PAGE) and matrix-assisted laser desorption/ionization-time-of-flight mass spectrometry (MALDI-TOF MS) with Autoflex Speed (Bruker Daltonics, Leipzig, Germany).

2.2.4 Incorporation of IgG-BAM conjugates onto cell membrane

The cancer cells (1×10^6 cells) were incubated in 100 μL of IgG-BAM solutions (1 μM in PBS) at room temperature for 15 min. As control experiments, cells were treated with IgG, BAM, or SF-25 solutions under the same condition, respectively. After treatment, the cells were washed twice with PBS. To evaluate the incorporation of IgG into the cell membrane, the IgG on the cell surfaces were fluorescently stained by Cy3-labeled anti-mouse Fc antibody according to standard protocols, and red-fluorescent cells were analyzed as Fc-positive cells by flow cytometry with a flow cytometer FACS Calibur using the CellQuest software (BD Labware, CA, USA). Additionally, the stained cells were observed with a confocal laser scanning microscope (CLSM) (TCS-NT, Leica Microsystems, Bensheim, Germany).

2.2.5 Generation of bone marrow-derived DCs

Bone marrow cells were obtained from female C57BL/6 mice (10 wk old, from Charles River Breeding Laboratories, Tokyo, Japan) in accordance with a protocol approved by the Animal Care and Use Committee of the University of Tokyo. After red cells were lysed with ACK lysing buffer (Lonza, NJ, USA), bone marrow cells were cultured at 1×10^6 cells/mL in RPMI medium (HyClone, UT, USA) in the presence of 20

ng/mL murine recombinant GM-CSF (rGM-CSF, Peprotech, UK). The cultures were fed by replacing 75% of the medium with a fresh rGM-CSF-containing medium on day 1 and 4. Non-adherent cells and weakly adherent cells on day 6 of culture were harvested by strong pipetting and used as DCs in the following experiments.

2.2.6 Phagocytosis of apoptotic HeLa cells by DCs

HeLa cells were fluorescently stained with 5- or 6-(N-Succinimidyloxycarbonyl)-fluorescein 3',6'-diacetate (CFSE; Dojindo, Kumamoto, Japan) for 5 min. These stained HeLa cells were irradiated with ultra-violet (UV) light for 5 min and incubated for 6 h to induce apoptosis. Then, to incorporate IgG into the cell membrane, apoptotic HeLa cells were treated with IgG-BAM as described above. As control experiments, apoptotic HeLa cells were also treated with BAM and SF-25. After treatment, apoptotic HeLa cells (2×10^5 cells) were co-cultured with DCs (1×10^6 cells) in 500 μL of RPMI medium. After co-culturing for 3 h, all cells were treated with a PE-conjugated anti-CD11c antibody for fluorescently-staining DCs. The cells were observed with CLSM and quantitatively analyzed using FACS, as described above. The cells possessing both green and red fluorescence were identified as the DC phagocytizing apoptotic HeLa cells [25]. The phagocytosis rate of the DCs was determined by calculating the ratio of the double fluorescent-positive cells to the total red fluorescent-positive cells.

2.3 Results and discussion

2.3.1 Optimization of random IgG-BAM conjugation

The process of conjugating IgG and BAM was optimized by changing the final molar ratio of BAM to IgG. The BAM molecule has an amine-reactive group at the end of the PEG chain and opposite to the lipid moiety, and reacts with lysine residues on IgG. Such random amine-coupling reactions onto IgG had been extensively used as a standard modification method because of their simplicity [26,27]. In the context of medical applications of PEGylated IgGs, the effects of random PEGylation on the effector function of IgG have been studied. Many studies using IgG modified with PEG of several kDa showed that FcγR binding to IgG was inhibited at high conjugation ratios of PEGs per IgG [26]. Therefore, to minimize the inhibition of FcγR binding by attachment of BAM, the condition of IgG-BAM conjugation was optimized by searching for a suitable conjugation ratio of BAM per IgG. The degree of attachment of BAM to IgG was qualitatively analyzed by SDS-PAGE (Figure 2-2A). As the molar ratio of BAM to IgG increased, the two bands derived from the heavy and light chains of IgG shifted to higher-molecular-weight species and broadened (Figure 2-2A, lanes 5~7), and finally, at the IgG:BAM ratio of 1:50, the bands of IgG disappeared and barely migrated onto the SDS-PAGE (Figure 2-2A, lane 8). In a previous report, a similar shift and broadening was observed in the band patterns of IgG modified with 5-kDa PEGs, and these changes were shown to correspond to the degree of PEG attachment [28]. Furthermore, MALDI-TOF MS analysis showed that IgG-BAM conjugation at the IgG:BAM ratio of 1:5 yielded IgGs with zero, one and two PEGs per IgG (Figure 2-2B). At that of 1:20, a broaden peak was observed around the molecular weight of IgG with from one to five PEGs per IgG in

the MS spectrum (Figure 2-2B, bottom). Thus, the present result indicates that IgGs bearing various amounts of BAM were successfully prepared by changing the molar ratio of BAM to IgG from 1 to 50.

2.3.2 Incorporation of IgG-BAM conjugates onto the cell membrane

Incorporation of IgG-BAM conjugates onto the membrane of cancer cells was confirmed by flow cytometer analysis. HeLa cells treated with IgG-BAM conjugates were stained with a fluorescent-labeled anti-mouse Fc antibody, and then, the ratio of Fc-positive cells was determined by flow cytometry. Compared with the control cells (treated with only IgG), the Fc-positive ratios of the cells treated with IgG-BAM conjugates effectively increased (Figure 2-3A). In particular, treatment with the IgG-BAM conjugated at the IgG:BAM ratio of 1:20 gave the largest Fc-positive ratio, up to ~90%. Similarly, CLSM observations clearly indicated that IgG-BAM conjugates at high conjugation ratios of BAM could effectively incorporate into the cell membrane (Figure 2-3B).

On the other hand, although the IgG-BAM conjugated at the IgG:BAM ratio of 1:50 should bear the largest amount of BAM, the Fc-positive ratio was inclined to be smaller than that conjugated at the IgG: BAM ratio of 1:20 ($p < 0.08$). This is probably because the binding of fluorescent-labeled anti-Fc antibody to IgG was inhibited with the conjugated BAM at high conjugation ratios of BAM per IgG. As described above, in the case of random PEGylation of IgG, similar inhibition was found to be dependent on the conjugation ratio [26]. In addition, when the BAM modified near the Fc domain of antibody was inserted into the cell membrane, the fluorescent-labeled anti-Fc antibody would be unable to approach the Fc domain because the Fc domain was buried in cell

membrane. The use of high conjugation ratios of BAM per IgG may increase the chance of modification near the Fc domain with BAM, thereby blocking the interaction with the anti-Fc antibody. From these results, I performed further experiments using the IgG-BAM conjugate prepared at the IgG:BAM ratio of 1:20.

To demonstrate the versatility of the present method, a large variety of cell lines including HepG2, Ba/F3 and B16 were treated with the IgG-BAM conjugate. I selected HepG2 as a second human adenocarcinoma, Ba/F3 as a non-adherent cell and B16 as a murine cancer cell. Figure 2-4 shows that the Fc-positive ratios of all treated cell lines were almost 100%, whereas those of the cells treated with intact IgG were <30%. From this result, the IgG-BAM conjugate was successfully incorporated into the cell membrane through the interaction between BAM and the cell membrane, regardless of the cellular characteristics such as cellular derivation and adhesion properties. This is because the dioleyl moiety of BAM interacts with the ubiquitous lipid bilayer of cells.

The efficiency of the presentation of Fc on the cell surface was almost the same between IgG-BAM and the tumor-specific monoclonal antibody SF-25 (Figure 2-4). SF-25 was reported to bind a wide range of human cancer cell lines [29]. As such, the use of specific IgG against a ubiquitous antigen on cancer cells may be applied in the preparation of ATC-IgG complexes and be effective against a wide range of tumors. However, such antigen-specific monoclonal IgGs have limited medical applications. Particularly, antigen-specific monoclonal IgGs are obtained from animals including mouse, rabbit and goat. Therefore, the humanization of the IgG is required to avoid immune activation in patients and for enhancing effector cell activation [30]. In contrast, using the present BAM-conjugation method, arbitrary human IgGs obtained from blood can be employed. Thus, IgG-BAM is a promising tool for supplying safe ATC-IgG complexes at a low cost.

2.3.3 Effects of incorporated IgG-BAM on phagocytosis by DCs

To evaluate whether treatment of IgG-BAM can enhance the uptake of ATCs by DC, the rate of phagocytosis was analyzed after co-culturing the treated ATCs with immature DCs. The ATCs and DCs were stained with a green fluorogenic reagent, CFSE, and a red fluorescent protein-conjugated anti-CD11c antibody, respectively. After co-culturing, the cells possessing both green and red fluorescence were identified as the DCs that had phagocytized ATCs [25], and such double-positive cells were observed with CLSM and quantitatively analyzed using flow cytometry (Figure 2-5). Figure 2-5A shows the CLSM image of the DCs cocultured with the ATCs treated with IgG-BAM. In the red-fluorescent image, the outer membrane of the DCs was stained red due to the attachment of the PE-conjugated anti-CD11c antibody. In contrast, in the green image, the whole ATCs fluoresced green. In the merged image, several red-stained cells were observed to have incorporated green-stained bodies. Consequently, the florescent images clearly confirm that DCs have phagocytized ATCs.

Figure 2-5B shows the phagocytosis rate of DCs under various conditions of treatment for ATCs. Compared with no treatment, treatment with IgG-BAM increased the phagocytosis rate more than two-fold. For over forty years, PEG has been commonly used as an effective fusogenic reagent for somatic cells [31]. As a control experiment, I investigated the effect of treatment with only BAM on the uptake of ATCs. Treatment with only BAM slightly increased the phagocytosis rate (Figure 2-5B). These results strongly suggest that the enhancement effect of IgG-BAM is not derived from the fusogenic properties of the PEG moiety but from the effective presentation of IgG on the ATC surface. In a previous report on ATC chemically-modified IgG, the phagocytosis rate

was enhanced almost two-fold by IgG modification [17]. Thus, the present enhancement of DC phagocytosis by IgG-BAM treatment is essentially the same as that observed when IgG is chemical modified. However, in contrast to chemical modification approaches, the present IgG-BAM treatment has the distinct advantage of enhancing phagocytosis without altering any chemical structures on the cell-surface antigens. There are many well-known cell surface antigens present on tumor cells, such as MUC-1 and CCA-1. Alteration in the chemical properties of such cell surface antigens may lead to decreases in the repertoire of antigenic epitopes for presentation to anti-tumor effector and mediator cells. On the other hand, the rate of intracellular processing of antigen remained virtually unaffected by the presence of IgG or PEGylated lipids on the antigen surface [32,33,34]. Thus, noncovalent treatment with IgG-BAM is a promising method for activating a broad repertoire of anti-tumor immunocytes.

As shown in Figure 2-5 , the enhancement effect when using IgG-BAM was almost the same as observed for SF-25. Since IgG-BAM incorporates anywhere on the surface of the lipid bilayer of ATCs, the amount of presented IgG on ATCs is presumably limited only by the surface area of the ATC, whereas the binding amount of Ag-specific IgG, such as SF-25, is limited by the surface amount of Ag. Thus, treatment with IgG-BAM has the potential advantage of presenting a relatively large amount of IgG on the cell surface. Conversely, IgG-BAM potentially has a disadvantage in its immunological effector activities. As described above, random PEGylation of IgG has been reported to decrease the effector activities of IgG through interfering with FcγR binding [26,35]. Presumably, random BAM modification similarly interferes in the interaction between the Fc domain on ATCs and the FcγR on DCs. In the present study, treatment with IgG-BAM may exert an enhancing effect that was comparable with SF-25. This is probably because

optimization of the BAM-conjugation condition minimized the disadvantage of IgG-BAM in the mean affinity with FcγR, and the advantage in the presentation amount countered this potential disadvantage.

2.4 Conclusion

In this chapter, I prepared IgG-BAM via random amine-coupling reaction. Random amine-coupling reaction is a standard modification method to attach molecules onto IgG, however, as shown in previous studies, random and high conjugation ratios of PEGs per IgG inhibit the effector function of IgG such as interaction between FcγR. Therefore, I tried to minimize the inhibition of Fc-FcγR interaction by searching for a suitable conjugation ratio of BAM per IgG. As a result, I concluded that the IgG:BAM ratio of 1:20 is the optimal condition to prepare IgG-BAM conjugation via random amine-coupling reaction. Next, cancer cells were treated with random IgG-BAM conjugate and the result indicated that by using random IgG-BAM conjugate, arbitrary IgG were successfully modified on cancer cell surfaces regardless of the cellular characteristics. Furthermore, ATCs treated with random IgG-BAM conjugates were more efficiently phagocytosed by DCs than untreated ATCs ex vivo. This result is consistent with a previous report on ATC chemically-modified IgG, which the phagocytosis rate was enhanced almost two-fold by IgG modification. In addition, this enhancement rate of treatment with IgG-BAM was essentially identical to the treatment rate with an Ag-specific IgG. This result indicates that IgG-BAM treatment enhances the efficacy of ATC-based DC vaccinations without the requirement of an expensive Ag-specific IgG. Theoretically, unlike Ag-specific IgG, since IgG-BAM incorporates anywhere on the

surface of the lipid bilayer of ATCs, the amount of IgG presented on ATCs is not limited by the surface amount of Ag. Thus, treatment of cancer cells with IgG-BAM conjugates has the potential advantage to induce stronger reaction between dendritic cells by displaying larger amount of Fc. However, the effect was only about two-fold compared to no treatment. Although I optimized the condition of amine-coupling reaction, still it is concerned that interaction between Fc and FcγR might be disturbed by some BAM attached to lysine residue of Fc regions, since lysine residues present in the structure were uniformly distributed on the Fab and Fc regions. Therefore, it is assumed that by investigating the reaction between IgG and BAM, ATCs might be phagocytosed by DCs more efficiently. To maximize the effect of IgG-BAM conjugate on DC immunotherapy, BAM must attach to IgG at the site which may not disturb the interaction between Fc and FcγR and this could be achieved by site-specific conjugation of IgG and BAM.

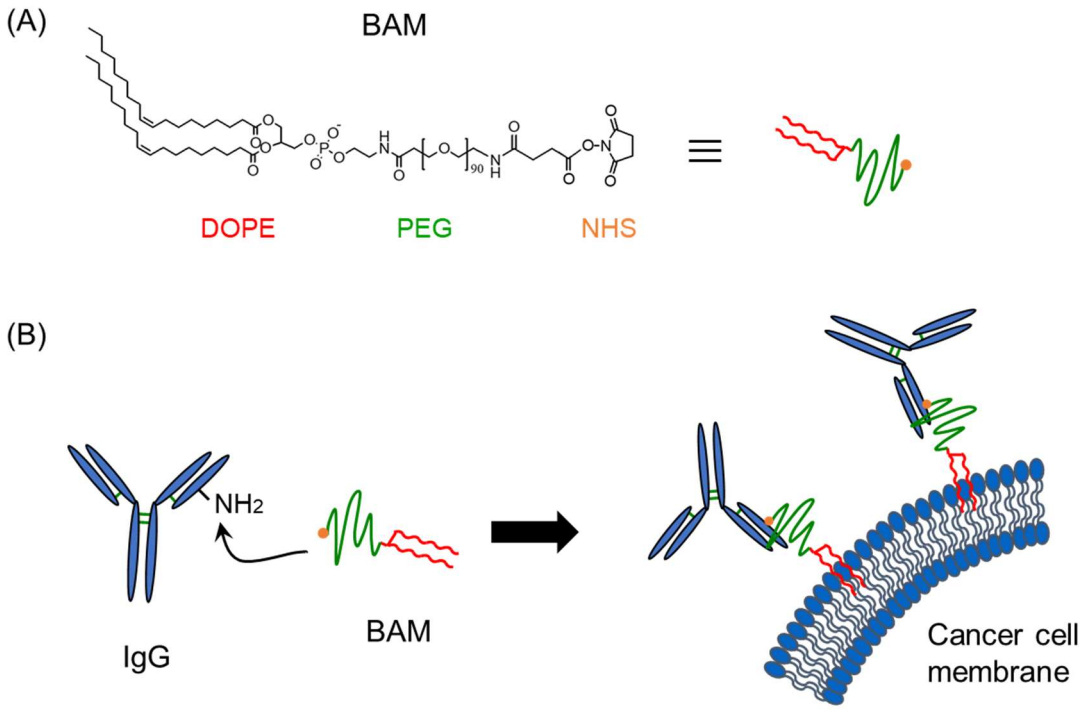

Figure 2-1. (A) Chemical structure of BAM used in chapter 2. (B) Schematic diagram of the incorporation of BAM-conjugated IgG into the cell membrane.

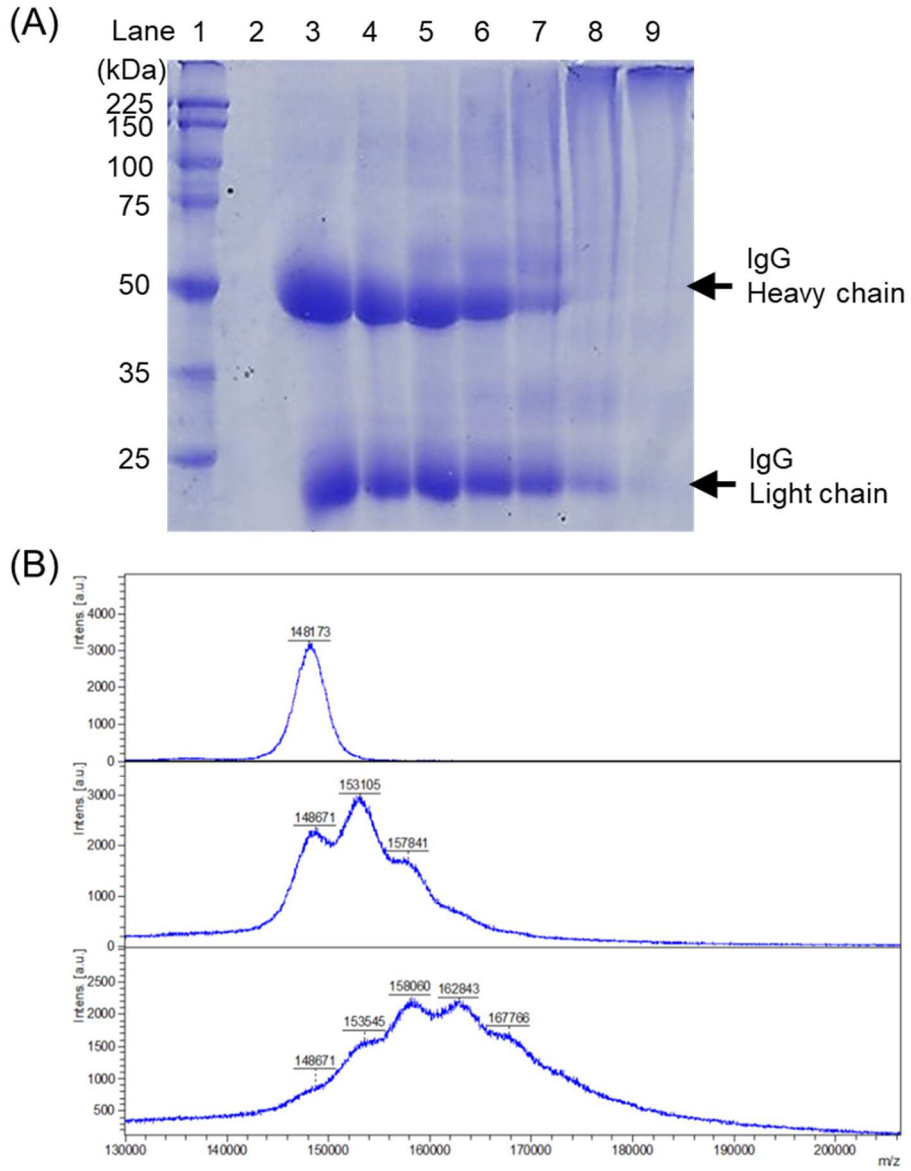

Figure 2-2. Optimization of the condition of IgG-BAM conjugation by changing the final molar ratio of BAM to IgG. (A) Qualitative analysis of the attachment of BAM to IgG by a reducing 7.5% polyacrylamide SDS-PAGE gel stained with Coomassie brilliant blue. Lane 1, protein molecular weight markers in kDa; lane 2, BAM as a control; lane 3, IgG as a control; lanes 4-9; IgG treated with BAM at various ratios: 1:1, 1:5, 1:10, 1:20, 1:50 and 1:100. (B) MALDI-TOF MS spectra of intact IgG (top), IgG treated with BAM at the IgG:BAM ratio of 1:5 (middle) and 1:20 (bottom).

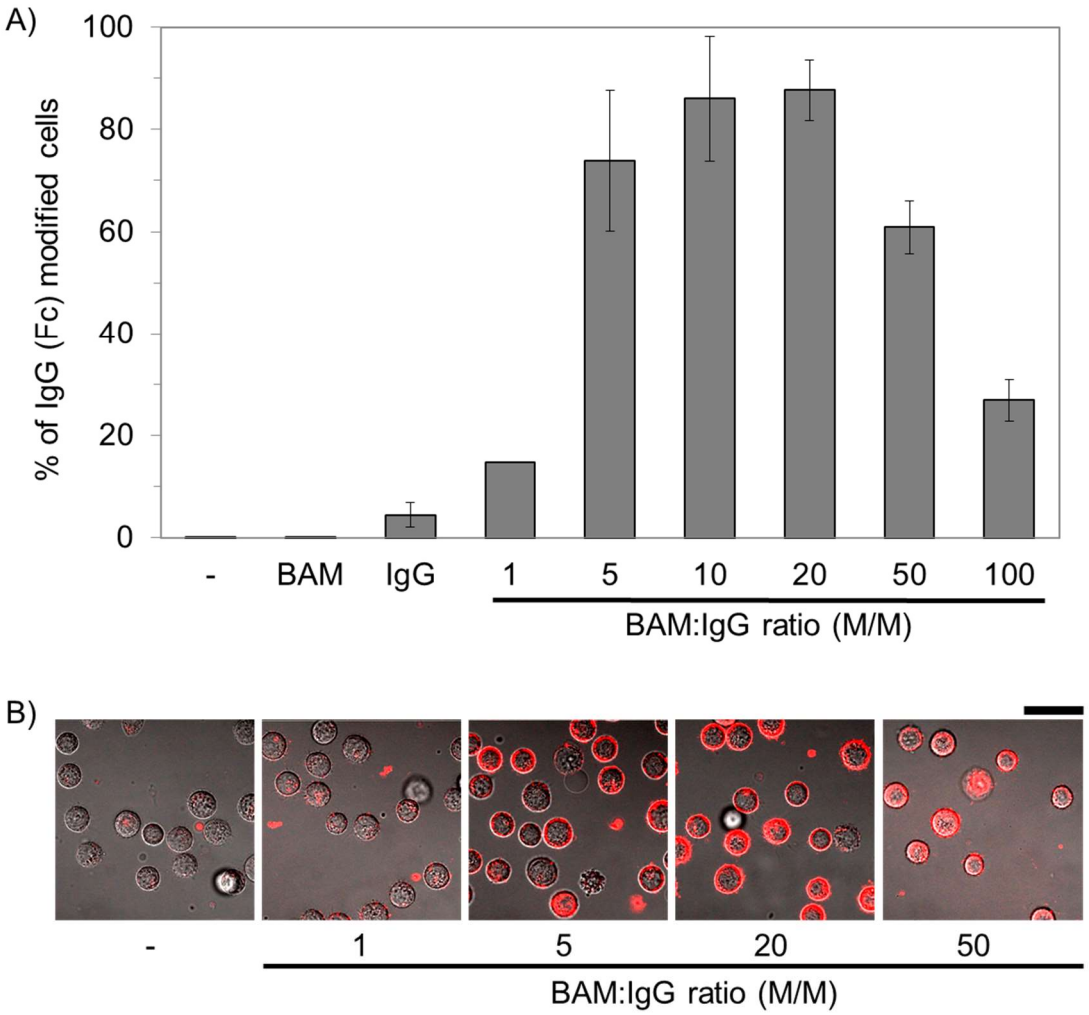

Figure 2-3. Optimization of the condition of IgG-BAM conjugation by changing the final molar ratio of BAM to IgG. HeLa cells were treated with IgG-BAM conjugates prepared in various conditions and stained with PE-labeled anti-Fc antibody. (A) Qualitative analysis of the incorporation of IgG-BAM conjugates into the membrane of HeLa cells by flow cytometry (n = 3). (B) CLSM observation. Bar = 40 μm.

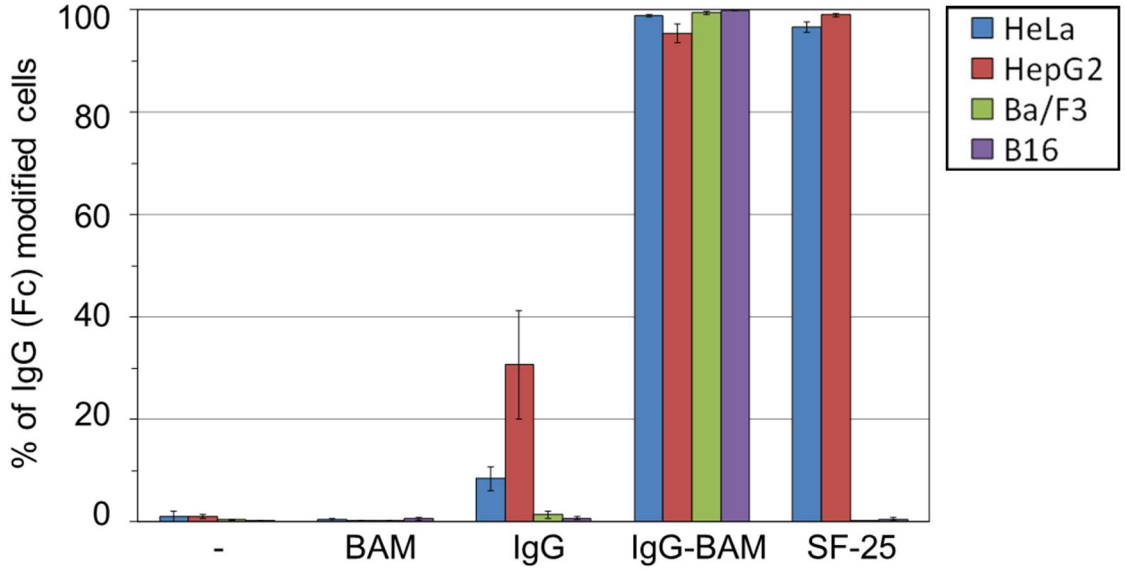

Figure 2-4. FACS analysis of Fc-positive ratios of various cell lines treated with IgG-BAM conjugate. Fc domains of IgG were stained with fluorescent-labeled anti-Fc antibody. Each data point represents the mean ± S.E. (n = 3).

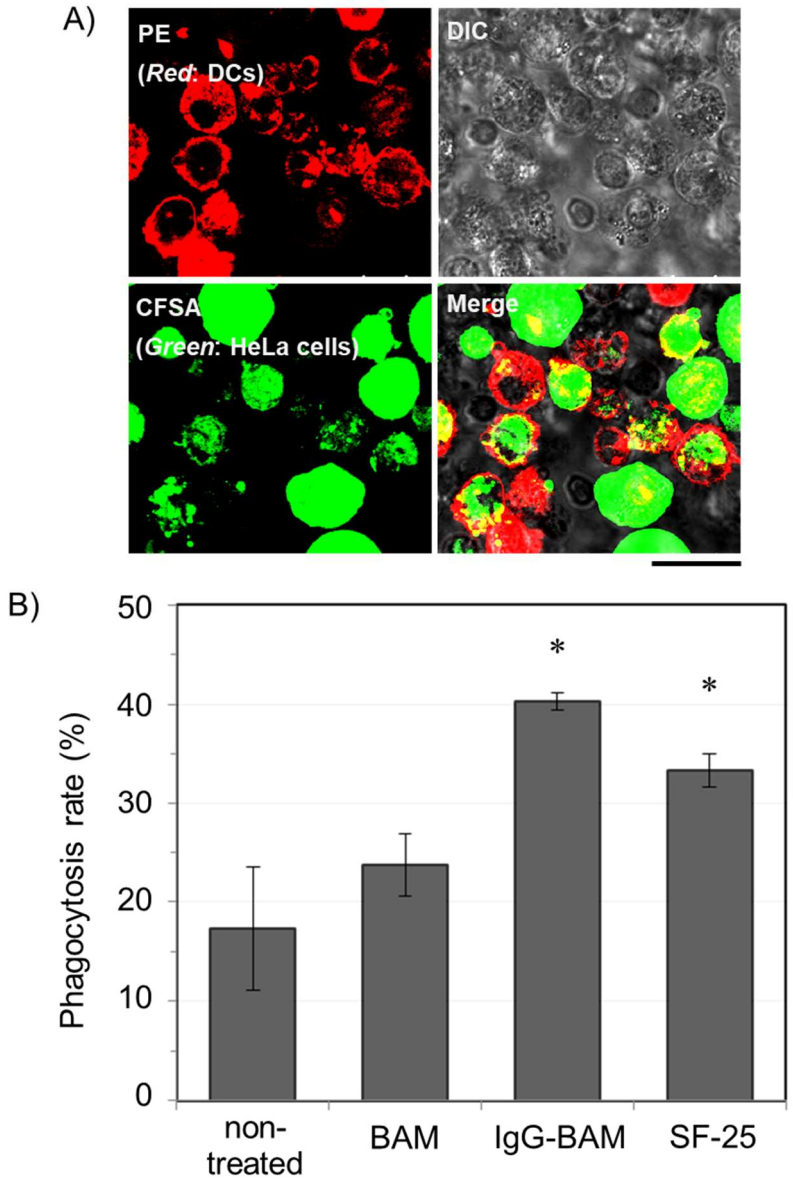

Figure 2-5. Analysis of the effects of the incorporated IgG-BAM on phagocytosis by DCs. Apoptotic HeLa cells and DCs were stained with CFSE and PE respectively. Apoptotic HeLa cells were treated with BAM, IgG-BAM conjugates or SF-25 antibody, and then, co-cultured with DCs to induce phagocytosis. (A) CLSM image of the DCs co-cultured with the apoptotic HeLa cells treated with IgG-BAM. Bar = 20 μm. (B) The ratio of DC phagocytizing apoptotic HeLa cells analyzed by flow cytometry. ($n = 3$, * $p < 0.05$ vs non-treated (student's t-test)).

Chapter 3. Studies on *in situ* enzymatic site-specific Fc-BAM conjugate and application to dendritic cell therapy

3.1 Introduction

Random IgG-BAM conjugate studied in previous chapter enhanced DC phagocytosis of apoptotic cancer cells. However, the effect was not enough, presumably because interaction between Fc and FcγR might be disturbed by some BAM attached to Fc region randomly. Therefore, in this chapter, I studied on site-specific IgG-BAM conjugation which may not disturb Fc-FcγR interaction to improve the efficacy of DC immunotherapy.

For site-specific lipidation, chemical [36, 37] and chemoenzymatic strategies [38, 39] are now available. For example, a model fluorescent protein was incorporated into the membrane of living cells through enzymatic site-specific lipidation [38]. However, conventional site-specific lipidation methods require the coexistence of amphiphilic reagents such as polar organic cosolvents and detergents that suppress aggregation of lipidated proteins *in vitro* [37-39]. Depending on the kind of protein and target cells, the usage of amphiphilic reagents may lead to protein denaturation or cytotoxicity.

In this study, site-specific modification of proteins was performed via sortase A (SrtA, EC 3.4.22.70)-mediated transpeptidation reactions. Among the family of transpeptidases, the Staphylococcus aureus SrtA is the most extensively used enzyme for *in vitro* site-specific linkage of proteins with synthesized compounds in various applications [40, 41]. This enzyme recognizes substrates that contain an LPXTG sequence, where X is a variable amino acid, and cleaves the amide bond between T and G, resulting in the formation of the thioester intermediate with the carboxyl group of T at the active-site cysteine. Successively, this thioester intermediate undergoes nucleophilic attack by an N-terminal amino group of the oligoglycine substrates, thereby producing

ligated products. Here, the peptide including the triglycine sequence at the N-terminus (GGGYC) was introduced onto the cell surfaces by conjugation with BAM. The GGGYC peptide was modified with BAM via thiol-maleimide chemistry (Figure 3-1A). Accordingly, Fc domains of IgG bearing a LPETG sequence at their C-terminus were prepared, and then reacted with the triglycine moiety of the peptides displayed on cancer cells through the SrtA-mediated transpeptidation (Figure 3-1B).

3.2 Materials and methods

3.2.1 Preparation of the GGGYC-BAM

A maleimidyl PEG-lipid, consisting of DOPE, PEG of 90 units and maleimide (MAL-BAM) was a gift from NOF Corporation (Tokyo, Japan). A pentapeptide with the sequence Gly-Gly-Gly-Tyr-Cys (GGGYC) was synthesized by standard Fmoc solid-phase peptide synthesis and purified by reversed-phase high-performance liquid chromatography (RP-HPLC). The GGGYC pentapeptide with a calculated mass of 454.2 Da was identified by MALDI-TOF MS at mass-to-charge ratios (*m/z*) of 455.4 for $[M + H]^+$ and 477.4 for $[M + Na]^+$. The GGGYC peptide was modified with MAL-BAM through a thiol-maleimide Michael addition in a MOPS buffer (20 mM, pH 7.0) including 5% DMSO. In the reaction mixture, the final concentrations of the GGGYC peptide and MAL-BAM were 1 and 5 mM, respectively. The reaction mixture was incubated overnight at room temperature. The reaction mixture was incubated for overnight at room temperature. The disappearance of free GGGYC peptide after incubation was confirmed by RP-HPLC analysis (Figure 3-2). The reactant was abbreviated as GGGYC-BAM.

3.2.2 Expression and purification of proteins

PrimeSTAR Max DNA polymerase (Takara Bio Inc., Shiga, Japan) was used for PCR, and all PCR-amplified sequences were verified by DNA sequencing. Sortase A (SrtA) was expressed and purified by following previous report [42]. The enhanced green fluorescent protein (EGFP) bearing a Leu-Pro-Glu-Thr-Gly (LPETG) sequence and a hexahistidine tag at the C-terminus ($EGFP_{-LPETG}$) was expressed and purified as follows. First, the expression plasmid for $EGFP_{-LPETG}$ was constructed as follows: The gene encoding $EGFP_{-LPETG}$ was obtained by PCR from pEGFP-N1 (Clontech Laboratories, Inc., CA) using the forward primer (5'-CGCGCGCCAT GGTGAGCAAG GGCGAGGAG-3') and the reverse primer (5'-CGCGCGGATC CCGACCAGTT TCAGGAAGCT TGTACAGCTC GTCCATGCCG-3'), and was subcloned into the NcoI/BamHI sites of pET-32b(+) (Novagen, Inc., Madison, WI, USA) to yield pET32b-$EGFP_{-LPETG}$. This expression plasmid was then transformed into E. coli BL21 Star(DE3) pLysS cells. The cells were grown in LB medium to an OD (600 nm) value of 0.7 at which time expression of the protein was induced by the addition of isopropyl-β-D-thiogalactopyranoside (IPTG) to a final concentration of 1.0 mM. After growth for an additional 16 h at 27°C, the cells were harvested by centrifugation. The cell pellets were resuspended in 50 mM Tris-HCl pH 7.5, 150 mM NaCl and lysed by sonication. $EGFP_{-LPETG}$ was purified from the soluble fraction of the lysate using Ni-NTA columns (HisTrap FF crude column; GE Healthcare, Waukesha, WI, USA) equilibrated with 50 mM Tris-HCl pH 7.5, 150 mM NaCl and 20 mM imidazole. $EGFP_{-LPETG}$ was eluted from the column with a linear gradient of imidazole (20-500 mM). The fractions containing $EGFP_{-LPETG}$ were collected and concentrated by ultrafiltration using Amicon Ultra-50 filter units (50 kDa molecular weight cut-off (MWCO); Millipore, Billerica, MA, USA). The concentrated protein was

subjected to anion exchange chromatography on a Hi-Trap Q FF crude column (GE Healthcare). The protein was eluted with a linear gradient of NaCl (150-500 mM). The fractions containing the protein were collected, and the thioredoxin tag derived from the pET32b vector was removed using enterokinase (EK Max; Invitrogen, Carlsbad, CA, USA). Ten units of EK Max were added to the fractions containing the protein and incubated at 4°C for 16 h, and the mixture was concentrated by ultrafiltration using an Amicon Ultra-30 filter unit (30 kDa MWCO; Millipore). The concentrated protein was subjected to gel-filtration chromatography on a Hi-Load Superdex 16/60 pg column (GE Healthcare), pre-equilibrated with 50 mM Tris-HCl pH 7.5 and 150 mM NaCl. The purified $EGFP_{\text{-LPETG-His6}}$ was concentrated with an Amicon Ultra-30 filter unit.

Expression vectors for the Fc domains of mouse IgG_1 and IgG_{2a} bearing a LPETG sequence and a hexahistidine tag at the C-terminus ($Fc1_{\text{-LPETG}}$ and $Fc2a_{\text{-LPETG}}$) were constructed as follows. The gene encoding $Fc1_{\text{-LPETG}}$ was obtained by PCR from cDNA extracted from SF25 (a mouse IgG_1 monoclonal antibody) expressing hybridomas using the forward primer (5′-GCCCTGCAGA GTGCCCAGGG ATTGTGG-3′) and the reverse primer (5′-CCGGCGGCCG CTCAATGGTG GTGATGGTGA TGTCCTCCGG TTTCAGGCAA TTTACCAGGA GAGTGGGAGA G-3′), and was subcloned into the PstI/NotI sites of pDisplay (Life Technologies, Gaithersburg, MD, USA) to yield $pDisp/Fc1_{\text{-LPETG}}$. The Fc1 ORF was identical to the GenBank accession no. FJ232993. The gene encoding $Fc2a_{\text{-LPETG}}$ was obtained by PCR from a synthesized DNA coding Fc2a (GenScript USA Inc., Piscataway, NJ, USA) using the forward primer (5′-GCCGCTGCAG ACCACGCGGC CCC-3′) and the reverse primer (5′-CCGGCGGCCG CTCAATGGTG GTGATGGTGA TGTCCTCCAG TTTCAGGCAA CTTCCCTGGT GTGCGAC-3′), and was subcloned into the PstI/ NotI sites of pDisplay to yield

pDisp/Fc2a-$_{LPETG}$. The Fc2a ORF was identical to the GenBank accession no. V00798. These expression vectors were transfected into Chinese hamster ovary (CHO) cells using the Lipofectamine™ LTX Reagent, with the PLUS™ Reagent (Life Technologies). Two days after transfection, the stable CHO clones producing Fc1-$_{LPETG}$ or Fc2a-$_{LPETG}$ were selected in G418 medium (1.2 mg/mL) for two weeks. Approximately 100 mL of culture medium was collected from each stable CHO culture dish. From the collected media, Fc1-$_{LPETG}$ and Fc2a-$_{LPETG}$ were purified using Ni-NTA columns (HisTrap FF crude column), equilibrated with 20 mM NaPi, 5 mM imidazole, pH 7.4. Fc1-$_{LPETG}$ and Fc2a-$_{LPETG}$ were eluted from the column with elution buffer (20 mM NaPi, 500 mM imidazole, pH 7.4), and the relevant fractions were dialyzed against PBS.

3.2.3 SrtA-mediated reaction in solution

50 μM of GGGYC-BAM was dissolved in a reaction solution, 50 μM EGFP-$_{LPETG}$ and 6 μM SrtA in the SrtA reaction buffer (50 mM Tris, 150 mM NaCl, 5 mM $CaCl_2$, pH 8.0). After incubation for 2 h at room temperature, this reaction mix solution was employed for SDS-PAGE analysis.

3.2.4 SrtA-mediated reaction on living cells

HeLa cells were cultured in Dulbecco's modified Eagle's medium (DMEM; Nissui, Tokyo, Japan) supplemented with 10% FBS, 2.05 mM L-glutamine, 30 μg/mL kanamycin and 0.2% $NaHCO_3$. Initially, the culture medium was removed from the dishes and HeLa cells were rinsed with PBS. The cells were then incubated in a GGGYC-BAM solution (50 μM, in PBS) at room temperature. After incubation for 15 min, cells were rinsed twice with PBS to remove any free GGGYC-BAM. Next, cells were incubated in a reaction

solution, 50 μM EGFP-$_{LPETG}$ and 6 μM SrtA in a SrtA reaction buffer (50 mM Tris, 150 mM NaCl, 5 mM $CaCl_2$, pH 8.0). After incubation for 2 h at room temperature, cells were rinsed twice with PBS to remove SrtA and free EGFP-$_{LPETG}$. As control experiments, without GGGYC-BAM treatment, intact cells were incubated in a reaction solution under the same condition, or cells treated with the GGGYC-BAM were incubated in a solution including only EGFP-LPETG or only SrtA. To evaluate the display of EGFP on cell membranes, the treated cells were observed with CLSM (LSM510; Carl Zeiss Co., Ltd, Germany) equipped with an Argon laser (488 nm).

For flow cytometry and SDS-PAGE analysis, cells must be transferred from culture dishes to plastic tubes. To avoid digestion of the displayed EGFP during the collection process, the cells were harvested before treatment with the GGGYC-BAM in the protocol described above. First, cultured HeLa cells were treated with 0.25% Trypsin-EDTA (Life Technologies) for 3 min at 37°C. Then, 1×10^6 collected cells were placed into a plastic tube and suspended into the GGGYC-BAM solution (50 μM). This was followed by incubation for 15 min. The treated cells were washed twice with PBS using centrifugation to harvest the cells. Next, cells were re-suspended into the reaction solution including SrtA and EGFP-LPETG, and incubated for 2 h, followed by two washing steps with PBS. Other detailed conditions were the same as described above. To quantitatively evaluate the display of EGFP on cell membranes, green-fluorescent-positive cells were analyzed as EGFP-positive cells by flow cytometry with a flow cytometer FACS Calibur using the CellQuest software (BD Labware, Franklin Lakes, NJ, USA).

3.2.5 SDS-PAGE and western blotting analysis

The reaction mixtures described in Section *3.2.3* and the lysates of the treated cells in Section *3.2.4* were fractionated by 12% SDS-PAGE. The SDS-PAGE gel was scanned with a Typhoon 9400 Scanner (GE Healthcare) using the excitation laser at 488 nm for EGFP-fluorescent imaging. For western blotting analysis, the fractionated proteins were electrotransferred from the SDS-PAGE gel onto a PVDF membrane. The blots were incubated with HRP-labeled anti-hexahistidine antibody (R&D Systems, Minneapolis, MN, USA) and stained using Chemi-Lumi One (Nacalai Tesque, Kyoto, Japan).

3.2.6 SrtA-mediated in situ reaction of $Fc_{\text{-LPETG}}$ and GGGYC-BAM on E.G7 cells

A murine thymoma cell line, E.G7 (EL-4 cells transfected with the chicken OVA cDNA) was kindly gifted by Prof. Tadatsugu Taniguchi at The University of Tokyo. E.G7 cells were cultured in RPMI1640 medium (Nissui, Tokyo, Japan) supplemented with 10% FBS, 2.05 mM L-glutamine, 30 μg/mL kanamycin and 0.2% $NaHCO_3$. E.G7 cells were irradiated with UV light for 5 min and incubated for 6 h to induce apoptosis. These non-adherent E.G7 cells were treated with the GGGYC-BAM as described in Section *3.2.4*. The treated cells were then re-suspended into the reaction solution including 6 μM SrtA and 50 μM $Fc_{\text{-LPETG}}$ ($Fc1_{\text{-LPETG}}$ or $Fc2a_{\text{-LPETG}}$), and incubated for 2 h, followed by two washes with PBS. Other detailed conditions were the same as described in Section *3.2.4*.

3.2.7 Phagocytosis of apoptotic E.G7 cells by DCs

The Fc-BAM treated apoptotic E.G7 cells were prepared as described in Section *3.2.6*. Apoptotic E.G7 cells (2×10^5 cells) were co-cultured with mouse bone marrow derived DCs (1×10^6 cells) in 500 μL of RPMI medium for 3 h at 37°C. When the co-

cultured cells were analyzed with a flow cytometer, apoptotic E.G7 cells were fluorescently stained with CFSE (Dojindo, Kumamoto, Japan) for 5 min before Fc-display treatment. After co-culturing, all cells were treated with a PE-conjugated anti-CD11c antibody for fluorescently-staining DCs. The cells were analyzed using FACS, as described in Section *2.2.6*.

3.2.8 Tumor-bearing mouse model

DCs for vaccination were prepared by co-culturing with apoptotic E.G7 cells as described above (Section *3.2.7*). C57BL/6 6 wk old female mice were immunized intraperitoneally with prepared DCs (1×10^6 cells in 100 μL PBS) on day 1 and day 7. At day 14, these mice were confronted subcutaneously with 5×10^4 E.G7 cells. Tumor sizes were measured every day after tumor injection. Tumor volume (V (mm^3)) was calculated using the formula: $V = 0.5 \times L \times W^2$, where L is the longest diameter and W is the shortest diameter in mm. Mice were ethically sacrificed when the tumor volume exceeded 2,000 mm^3.

3.2.9 In vivo cytotoxicity assay

C57BL/6 6 week old female mice were immunized with prepared DCs on day 1 and day 7 as described above (Section *3.2.8)*. E.G7 cells were fluorescently stained with CFSE and injected intravenously (1×10^7 cells in 100 μL PBS) on day 14. Four hours later, spleen cells were obtained and green-fluorescent-positive cells were analyzed as remaining CFSE-labeled E.G7 cells by FACS.

3.3 Results and discussion

3.3.1 Concentration-dependency of incorporation of BAM into cell membranes

First, the concentration-dependency of incorporation of BAM derivatives into cell membranes was investigated. Living cells were treated with a biotinylated BAM at various concentrations and then stained with fluorescent-labeled streptavidin, followed with analysis by flow cytometry. As a result, the fluorescence derived from the incorporation of biotinylated BAM was adequately saturated above their concentrations of 20 μM (Figure 3-3).

3.3.2 Concentration- and time-dependency of SrtA-mediated ligation on living cells

Next, to investigate the concentration- and time-dependency of SrtA-mediated ligation reaction on living cells, a fluorescent-labeled substrate peptide was ligated with GGGYC-BAM on living cells at various concentrations for various times. A peptide including the substrate sequence, GYGLPETGG was purchased from Toray Research Center Inc. (Otsu, Japan) and modified with Alexa Fluor 488 (AF488) succinimidyl ester (from Invitrogen, Carlsbad, CA, USA) through an amide coupling reaction. The reaction mixtures including this AF488-labeled GYGLPETGG peptide (0-100 μM) and 6 μM SrtA were added onto the harvested living cells previously treated with GGGYC-BAM. After incubation for various time periods (0-3 h), these cells were rinsed and analyzed with a flow cytometer. As a result, at all concentrations of substrate peptides, the mean fluorescence of the cells treated for 2 h was almost the same as that for 3 h (Figure 3-4). From these results, the SrtA-mediated ligation reaction on living cells was confirmed to reach equilibrium in 2 h.

3.3.3 SrtA-mediated in situ ligation of EGFP-$_{LPETG}$ with GGGYC-BAM on living cells

Subsequently, EGFP-$_{LPETG}$ was displayed on the surface of HeLa cells through the SrtA-mediated modification of BAM under optimal condition invested previously. Before the SrtA reaction, a conjugate of the GGGYC-BAM was incorporated into the cell membrane by simply dropping this solution onto the culture dish followed by incubation for 15 min. After removal of free GGGYC-BAM, both EGFP-$_{LPETG}$ and SrtA were added to the culture dish to perform the SrtA-mediated *in situ* ligation between EGFP-$_{LPETG}$ and the GGGYC-BAM. As shown in Figure 3-5A, the fluorescence of EGFP was clearly observed on the cell membrane after 2 h of the reaction and the removal of the free EGFP-$_{LPETG}$. Conversely, without SrtA, such EGFP fluorescence was not observed (Figure 3-5A). Furthermore, with SrtA, the EGFP fluorescence-positive ratio of living cells was 84%, whereas without SrtA, it was 1.2% (Figure 3-5B). Thus, EGFP was successfully displayed on living cells with high efficiency using the presented *in situ* method.

3.3.4 Confirmation of the site-specificity of EGFP and BAM ligation

To confirm the specific modification of EGFP with the GGGYC-BAM, the products of the SrtA-mediated reaction both *in vitro* and *in situ* were analyzed by SDS-PAGE and western blotting analysis. In the product of the *in vitro* reaction, a shifted green fluorescent band was detected above the band of intact EGFP-$_{LPETG}$ by fluorescent image analysis of the electrophoretic gel (Figure 3-6A, lane 6). In addition, this shifted band was not detected by western blotting analysis using an anti-hexahistidine tag antibody (Figure 3-6B, lane 6). Here, a hexahistidine tag was fused at the end of C-terminus of EGFP-$_{LPETG}$. Accordingly, these results strongly suggest that the shifted band was derived from the

BAM-modified EGFP, which bear a bulky PEG-lipid and lost the hexahistidine tag. Moreover, the same shifted band was detected from the lysate of the cells, in which the *in situ* SrtA-mediated modification was performed (Figure 3-6A, lane 10). Thus, by both *in vitro* and *in situ* modification, $EGFP_{\text{-LPETG}}$ was site-specifically modified with the GGGYC-BAM.

3.3.5 Effects of incorporated site-specific Fc1-BAM and Fc2a-BAM conjugates on phagocytosis by dendritic cells

LPETG-fused Fc domains of mouse IgG_1 and IgG_{2a} ($Fc1_{\text{-LPETG}}$ and $Fc2a_{\text{-LPETG}}$) were displayed on E.G7 cells through *in situ* SrtA-mediated modification. As is the case with $EGFP_{\text{-LPETG}}$, $Fc1_{\text{-LPETG}}$ and $Fc2a_{\text{-LPETG}}$ were successfully displayed on E.G7 cells, as confirmed by CLSM observation (Figure 3-7A) and FACS analysis after immunostaining (Figure 3-7B). These Fc domain-displayed E.G7 cells were co-cultured with immature DCs at 37°C. Figure 3-8 shows the phagocytosis rate of DCs under various conditions of treatment for E.G7 cells. Compared with no treatment or treatment with only the GGGYC-BAM, display of the Fc increased the phagocytosis rate, and especially, the phagocytosis rate was increased almost four-fold by displaying $Fc2a_{\text{-LPETG}}$. On the other hand, display of $Fc1_{\text{-LPETG}}$ led to only a slight increase in the phagocytosis rate; although the mean amounts of displayed Fc domains per cell were almost the same in the FACS analysis (Figure 3-7B). Among the IgG subclasses, IgG_{2a} are generally considered to be more active for immune effector responses than IgG_1 [43]. This is because IgG_1 strongly binds to both the activating and inhibitory FcγRs, whereas IgG_{2a} binds with low affinity to the inhibitory FcγR. In FcγR-mediated phagocytosis, IgG_1 cluster immune complex with the inhibitory FcγRIIb and dampen phosphorylated signals for initiating

phagocytosis via recruiting phosphatases on the immunoreceptor tyrosine-based inhibitory motifs (ITIM) of FcγRIIb [43, 44]. The present difference in the phagocytosis rates between $Fc1_{\text{-LPETG}}$ and $Fc2a_{\text{-LPETG}}$ is assumed to be derived from the properties of IgG_1 and IgG_{2a}, respectively.

3.3.6 Comparison between random and site-specific BAM conjugates

To compare the effect of random IgG-BAM conjugates and site-specific Fc-BAM conjugates, random IgG-BAM conjugate and site-specific Fc2a-BAM conjugate were displayed on E.G7 cells as described in Section *2.2.4* and Section *3.2.6,* respectively. As expected, modification of site-specific Fc2a-BAM conjugate induced phagocytosis more effectively than random IgG-BAM conjugate (Figure 3-8). This result suggests that site-specific ligation between Fc and BAM is an effective method to display Fc on ATCs without altering the interaction between FcγR on DCs.

3.3.7 Anti-tumor effect of site-specific Fc-BAM conjugate on DC vaccination

To investigate the anti-tumor effect of DC vaccine loaded with Fc domain-modified tumor cells, tumor cytotoxicity was evaluated. Mice were immunized twice with DCs phagocytizing E.G7 cells modified with Fc domains. Seven days after the second immunizations, CFSE-labeled E.G7 cells were injected intravenously. When the anti-tumor cytotoxicity were induced, immune cells will kill E.G7 cells and CFSE positive cell ratio in spleen cells will decrease. As a result of FACS analysis, CFSE-labeled E.G7 cell positive ratio was significantly decreased in spleen cells of the mice that were immunized with DCs pulsed with E.G7 cells displaying Fc2a-BAM (Figure 3-9). On the other hand, other mice that were immunized with DCs pulsed with Fc1-BAM treated

E.G7 or non-treated E.G7 showed slight deceases of CFSE-labeled E.G7 cells. This result indicates that DCs loaded with more ATCs induce stronger anti-tumor immunity.

Furthermore, the efficiency of Fc domain-modified tumor cells as a source for a DC vaccine was evaluated in tumor-bearing mouse model. Mice were immunized twice with DCs treated with various conditions and seven days after the second immunizations, these mice were confronted with E.G7 cells, and the size of tumor on each mouse was observed. As a result, inhibition of tumor growth was confirmed on the mice that were immunized with DCs pulsed with E.G7 cells displaying Fc2a-BAM, whereas mice treated with DCs pulsed with E.G7 cells displaying Fc1-BAM showed no significant protection against tumor growth (Figure 3-10). Again, this result indicates that the more ATCs loaded to DCs, the stronger anti-tumor immunity is induced even in the body. Hence, site-specific Fc2a-BAM conjugate has a potential to improve clinical responses in DC vaccines.

3.4 Conclusion

In this chapter, to conjugate BAM on IgG without inhibiting Fc-FcγR interaction, I investigated a novel method to conjugate specific site of Fc domain and BAM via enzymatic reaction of SrtA. Since SrtA-mediated transpeptidation reactions is a facile detergent-free enzymatic reaction, SrtA reaction exhibit low protein denaturation and cytotoxicity compared to conventional site-specific lipidation methods which require the coexistence of amphiphilic reagents such as polar organic cosolvents and detergents that suppress aggregation of lipidated proteins *in vitro*. First, I used EGFP as a tool protein to optimize the condition of the reaction and I succeeded to display EGFP on living cells with high efficiency by SrtA-mediated *in situ* ligation method. I also confirmed the site-

specific modification of EGFP and BAM by multiple method. Subsequently, I prepared LPETG-fused Fc domains of mouse IgG_1 and IgG_{2a} ($Fc1_{\text{-LPETG}}$ and $Fc2a_{\text{-LPETG}}$). Among the subclasses of mouse IgG, IgG_{2a} show stronger interaction than IgG_1 with FcγRI on DCs which is an active receptor for phagocytosis. Therefore, comparison of functions between Fc1-BAM and Fc2a-BAM indicate the difference of reaction between FcγR on DCs. Both Fc domain were successfully displayed at the same amount on cancer cells without aggregation under an amphiphilic reagent-free condition. Compared with no treatment, the phagocytosis rate was increased almost four-fold by displaying Fc2a-BAM. On the other hand, display of Fc1-BAM led to only a slight increase in the phagocytosis rate. As described above, since the activation of phagocytosis of DCs via Fc-FcγR interaction differ by the subclass of IgG, it is estimated that Fc domains displayed on ATCs interacted functionally with FcγR on DCs and therefore, induced strong phagocytosis. In addition, compared to randomly conjugated IgG-BAM prepared by the method described in Chapter 2, site-specifically conjugated Fc2a-BAM induced phagocytosis of ATCs by DCs more effectively, which again indicates the functional interaction of Fc2a and FcγR. Finally, *in vivo* anti-tumor effect of vaccination of the DCs which phagocytized various IgG(Fc)-BAM conjugate treated ATC were evaluated. As expected, site-specific Fc-BAM treated ATCs induced stronger tumor immunity and delayed tumor development in mouse. Altogether, these result suggest that combination use of SrtA and BAM to modify Fc on tumor cells has a potential to improve clinical responses of DC immunotherapy.

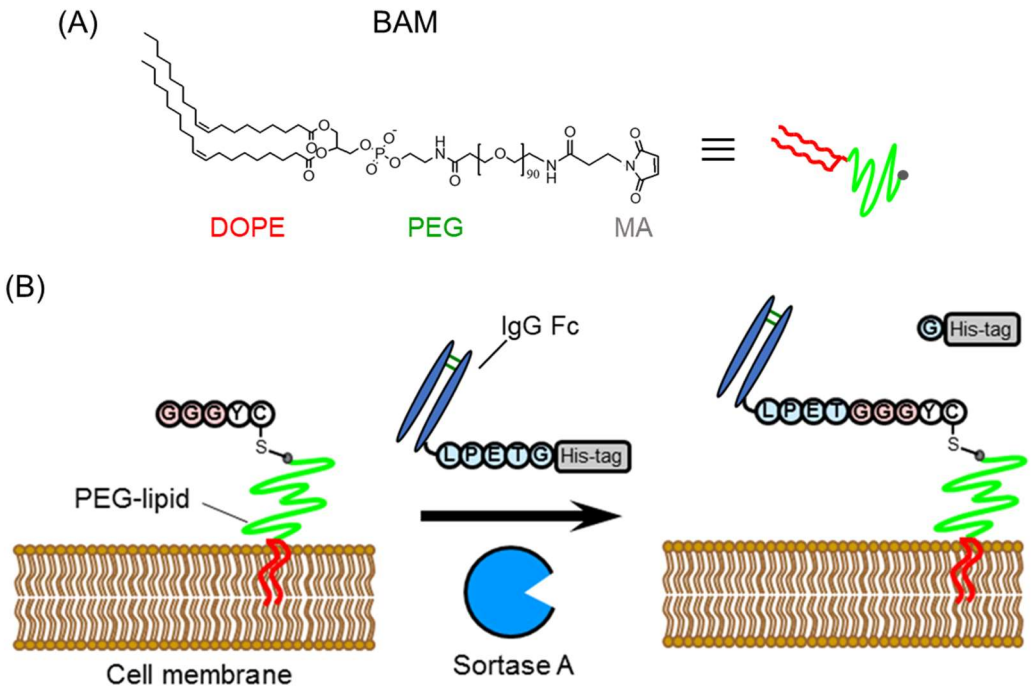

Figure 3-1. (A) Chemical structure of BAM used in chapter 3. (B) Schematic illustration of sortase A-catalyzed modification of a Fc domain of IgG with BAM presented on cell membranes.

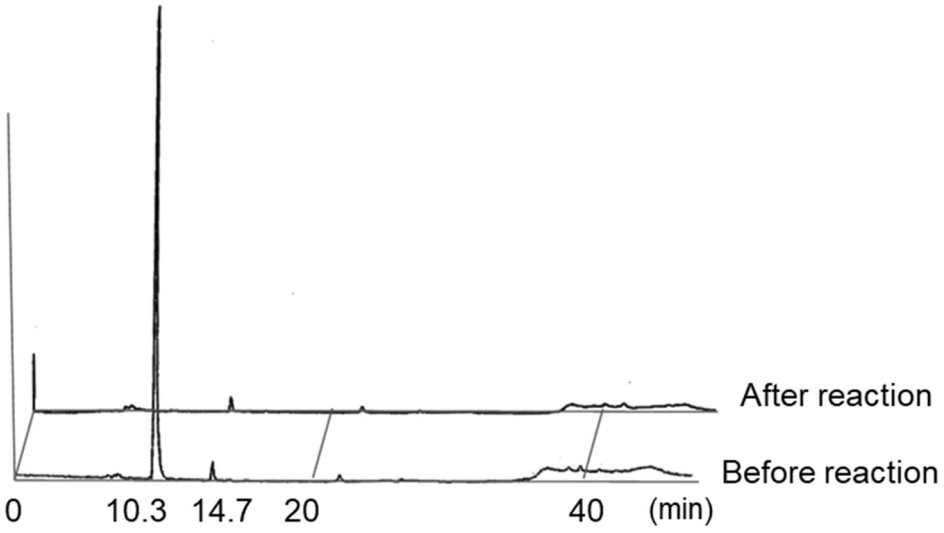

Figure 3-2. RP-HPLC chromatogram of a GGGYC peptide before and after reaction with maleimidyl BAM. The peak of peptide was detected by measuring the absorbance at 220 nm. Free GGGYC peptide was detected at 10.3 min.

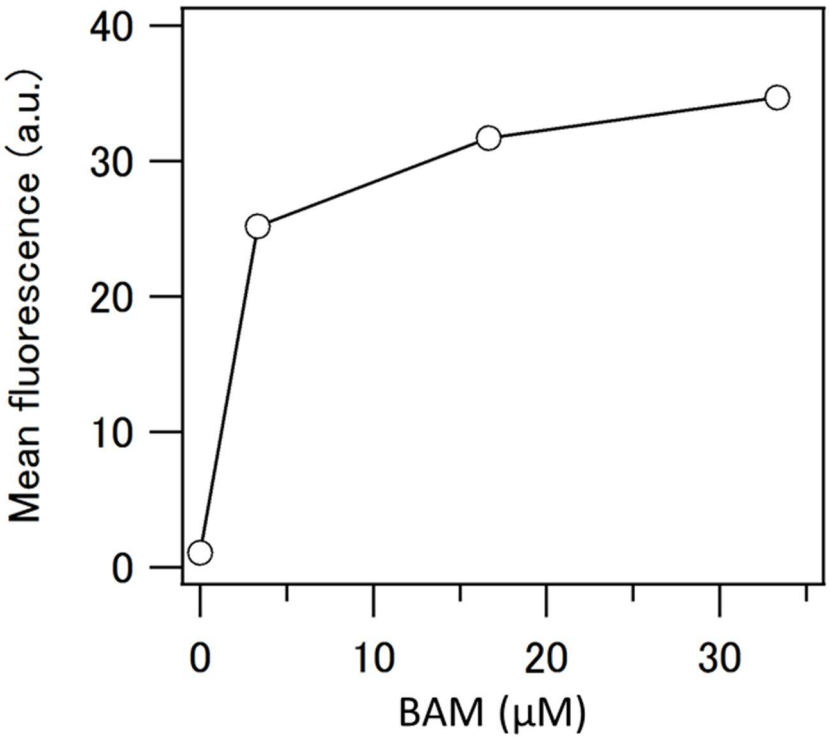

Figure 3-3. Incorporation of a biotinylated PEG-lipid onto living cells at various concentrations. The cells treated with biotinylated BAM for 15 min were stained with AF488-labeled streptavidin, followed with FACS analysis.

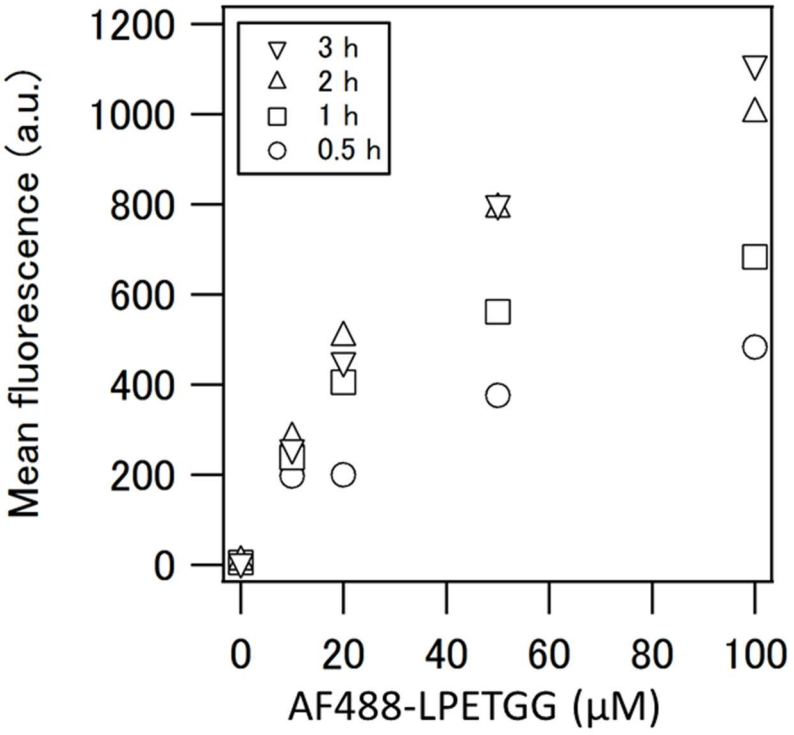

Figure 3-4. SrtA-modified ligation of an AF488-labeled substrate peptide with a PEG-lipid on living cells at various substrate concentrations for various time periods.

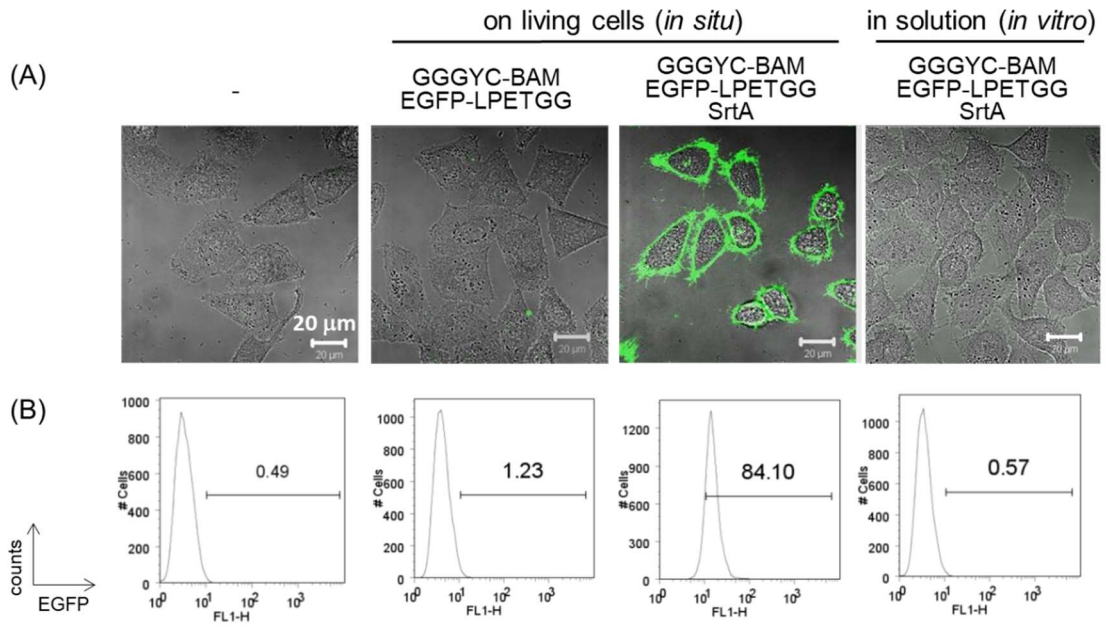

Figure 3-5. Sortase A-catalyzed modification of enhanced green fluorescent protein with BAM *in situ* and *in vitro*. HeLa cells were treated with GGGYC-BAM and successively with EGFP-$_{LPETG}$ with or without SrtA on living cells (*in situ*) or in solution (*in vitro*). (A) The fluorescent images merged with the bright-field images were obtained with a confocal laser scanning microscope. The scale bar is 20 μm. (B) Qualitative analysis of the incorporation of EGFP into the membrane of HeLa cells by flow cytometry. The number described in each FACS histogram indicates the green fluorescence-positive ratio of living cells.

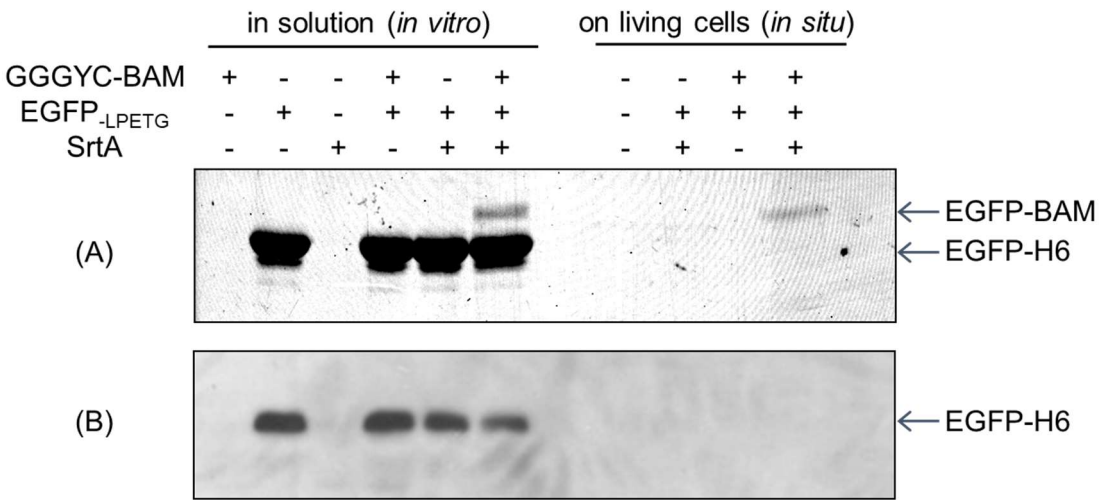

Figure 3-6. Confirmation of sortase A-catalyzed modification of EGFP with BAM *in vitro* or *in situ*. $EGFP_{-LPETG}$ and GGGYC-BAM were incubated with or without SrtA in solution (*in vitro*) or on living cells (*in situ*). The reaction solution (*in vitro*) or cell lysate (*in situ*) were loaded on SDS-PAGE gel and analyzed by fluorescent scanning (A) or western blotting with an anti-His-tag antibody (B).

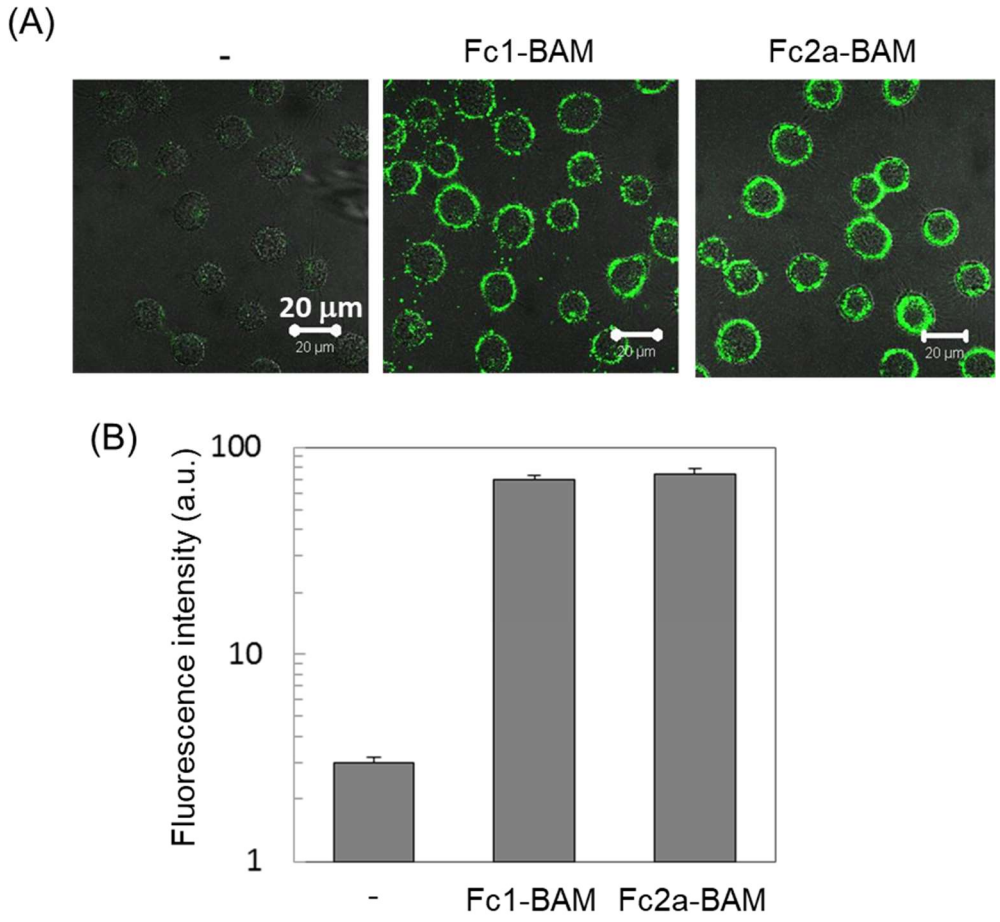

Figure 3-7. Sortase A-catalyzed modification of the Fc domains of mouse IgG_1 and IgG_{2a} on E.G7 cells. (A) Fluorescent microscopic images of living E.G7 cells, modified with the Fc domains of mouse IgG_1 (Fc1-BAM) and IgG_{2a} (Fc2a-BAM). The Fc domains were stained with a fluorescent-labeled anti-Fc antibody. The scale bar is 20 µm. (B) FACS analysis of E.G7 cells modified with the Fc domains of mouse IgG_1 (Fc1-BAM) and IgG_{2a} (Fc2a-BAM). The fluorescent intensity of the E.G7 cells modified with the Fc domains and stained by the fluorescent-labeled anti-Fc antibody. The fluorescent intensity correlates with the amount of the Fc domains modified on E.G7 cells. Each data point represents the mean ± S.E. (n = 3).

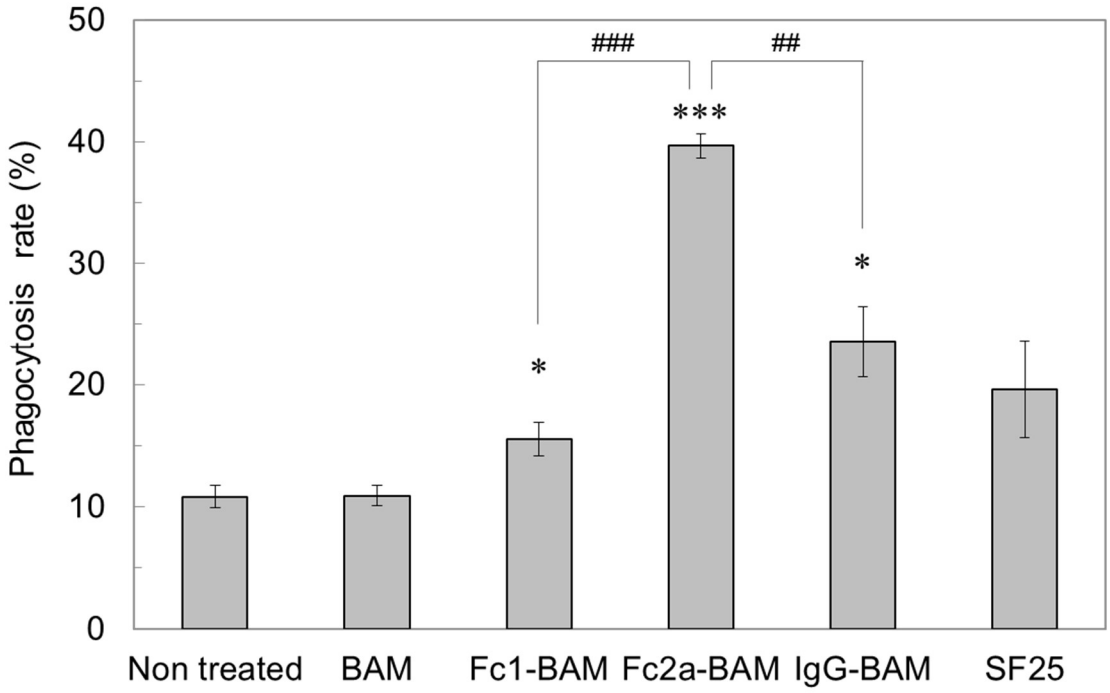

Figure 3-8. The phagocytosis rate of E.G7 cells treated with various combinations of the BAM, SrtA mediated site-specific Fc1-BAM and Fc2a-BAM conjugates, random IgG-BAM conjugates or tumor specific SF25 with DC. Each data point represents the mean ± S.E. (n = 3). *, *** $p < 0.05$, 0.001 vs non treated (student's t-test). ##, ### $p < 0.01$, 0.001 vs Fc2a-BAM (student's t-test).

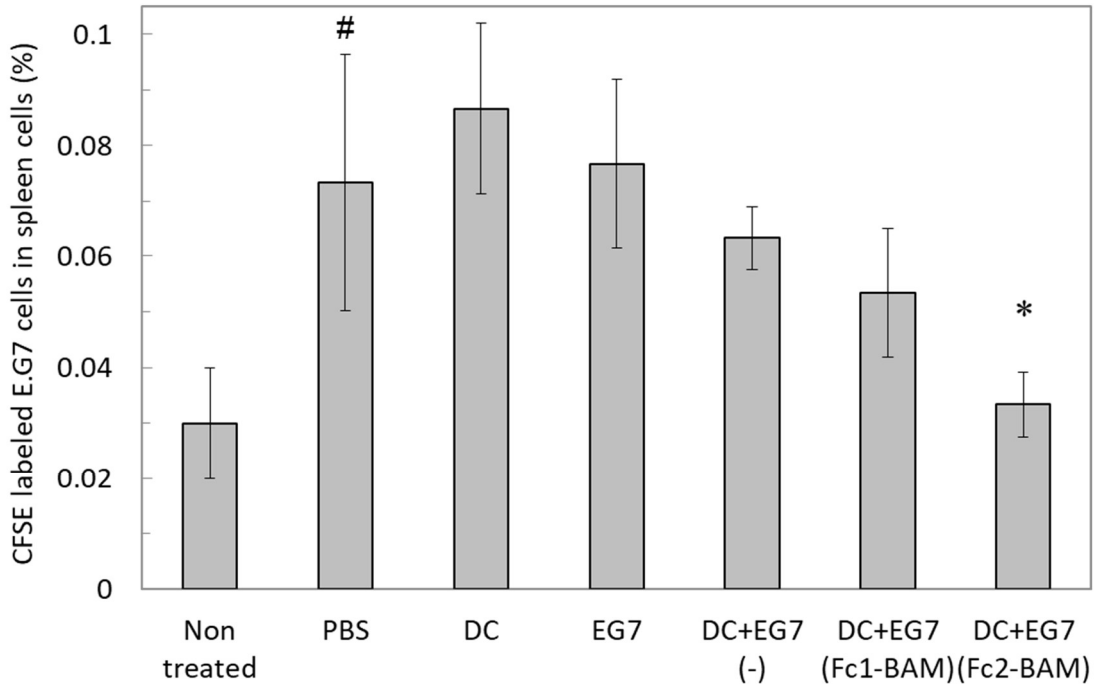

Figure 3-9. Analysis of tumor cytotoxicity of mice immunized with DCs prepared under various conditions. Mice were vaccinated with either PBS (PBS), DCs (DC), apoptotic E.G7 cells (E.G7[-]), DCs pulsed with non-treated apoptotic E.G7 cells (DC (E.G7[-])), DCs pulsed with Fc1-displaying apoptotic E.G7 cells (DC (E.G7[Fc1-BAM])) and DCs pulsed with Fc2a-displaying apoptotic E.G7 cells (DC (E.G7[Fc2a-BAM])). E.G7 cells were fluorescently stained with CFSE and injected intravenously 14 days after first vaccination. Four hours later, spleen cells were obtained and green-fluorescent-positive cells were analyzed as remaining CFSE-labeled E.G7 cells by FACS. Each data point represents the mean ± S.E. (n = 3). # $p < 0.05$ vs Non treated (student's t-test). * $p < 0.05$ vs PBS (student's t-test).

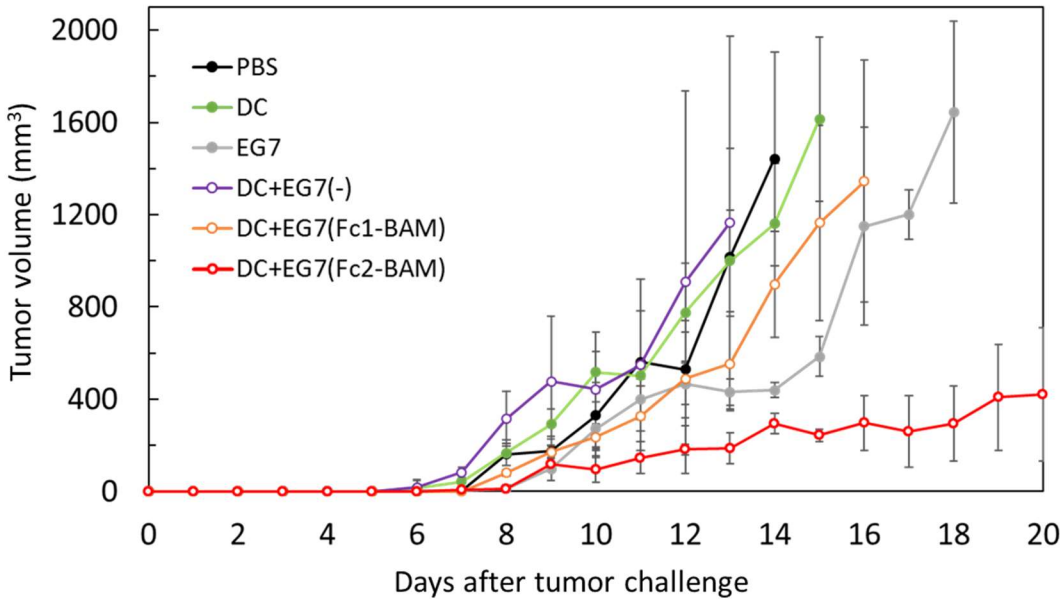

Figure 3-10. Volumes of tumor after the transplantation of E.G7 cells in the mice immunized with DCs. Mice were vaccinated with either PBS (PBS), DCs (DC), apoptotic E.G7 cells (E.G7[-]), DCs pulsed with non-treated apoptotic E.G7 cells (DC (E.G7[-])), DCs pulsed with Fc1-displaying apoptotic E.G7 cells (DC (E.G7[Fc1-BAM])) or DCs pulsed with Fc2a-displaying apoptotic E.G7 cells (DC (E.G7[Fc2a-BAM])). E.G7 cells were transplanted 14 days after first DC vaccination. Tumor volume was calculated using the formula: $V = 0.5 \times L \times W^2$, where L is the longest diameter and W is the shortest diameter in mm. Mice were ethically sacrificed when the tumor volume exceeded 2,000 mm^3. Each data point represents the mean ± S.E. (n = 3).

Chapter 4. General conclusion and perspectives

4.1 General conclusion

The main purpose of this study was to investigate the most efficient method to display arbitrary IgG on cancer cells with the application of BAM to improve the effect of DC immunotherapy.

In chapter 2, I studied on random IgG-BAM conjugate which showed successful modification of arbitrary IgG on various cancer cells. Although this randomly conjugated IgG-BAM by using amine-coupling reaction method was very simple and fast to prepare, it was very difficult to adjust a suitable conjugation ratio of BAM per IgG not to inhibit the effective interaction between IgG and FcγR. Indeed, ATCs treated with random IgG-BAM conjugates were more efficiently phagocytosed by DCs than untreated ATCs, however, the effect was only about two-fold compared to no treatment. Therefore, I hypothesized that by investigating the site-specific ligation of IgG and BAM, ATCs might be phagocytosed by DCs more efficiently.

Subsequently, in chapter 3, to conjugate BAM on IgG without inhibiting Fc-FcγR interaction, I studied on site-specific IgG(Fc)-BAM conjugate via enzymatic reaction of SrtA. This method was unique at the point to operate the ligation of BAM and Fc fragment on the cell surface. This method successfully conjugated Fc and BAM site-specifically and enhanced DC phagocytosis of ATCs more efficiently than random IgG-BAM conjugate by displaying functional Fc to FcγR on DCs. Furthermore, vaccination of the DCs which phagocytized site-specific Fc-BAM treated ATCs induced strong *in vivo* anti-tumor effect and delayed tumor development in mouse. These results strongly indicate that site-specific Fc-BAM treatment represents a promising method for opsonizing ATC with human arbitrary IgG(Fc), and that this approach will lead to objective clinical

responses in DC vaccines. Yet, there are lots of issues left to solve before clinical trial, such as, effect; is this method more efficient than conventional DC antigen loading method, side effect; is the carryover of SrtA, BAM and ATCs co-cultured with DCs safe to vaccinate. Further efforts will be required to approve site-specific Fc-BAM conjugate to clinical of DC immunotherapy.

4.2 Perspectives

In this study, the efficient method for displaying soluble proteins on living cells was successfully developed by employing both BAM and SrtA. The present *in situ* protein modification approach could fully resolve the conventional difficulties of protein lipidation caused by the aggregation-prone action of hydrophobic lipids. Recently, the similar lipidation approach with SrtA was reported as a protein modification on liposomes [45]. However, in this previously-reported work, a diglycine-modified PEG-lipid was mixed with the lipids in organic solvent for incorporating onto liposome, and the application of this method to living cells has not been reported yet. On the other hand, as mentioned in the review written by Dozier and Distefano, 2015 [46], present work is the first report demonstrating that SrtA-catalyzed *in situ* protein modification was achieved on living cells and is applicable to the modulation of a biological cell-to-cell interaction. Critical point of this achievement was the employment of a PEG-dioleyl derivative (BAM) as a biocompatible anchor for incorporating the substrate of SrtA onto the membranes of living cells. In addition, the high specificity of the SrtA-mediated reaction, which enables specific ligation under the coexistence of many other membrane proteins, was also necessary for the modification on cell surfaces.

Thus, the combined use of a BAM and SrtA represents a very effective and simple approach to display target proteins on living cells via exogenous transduction, particularly useful for difficult-to-transfect cells, and is a promising tool for regulating and reinforcing cell-cell interactions in cell and tissue engineering fields.

Acknowledgements

I would like to express my deep gratitude to Prof. Kouji Nakamura (Faculty of Life and Environmental Sciences, University of Tsukuba) for being in charge of this dissertation, and for his valuable guidance and encouragement during my Ph.D study. Also, I would like to express my sincere gratitude to Prof. Yingnan Yang (University of Tsukuba), Associate Prof. Kosumi Yamada (University of Tsukuba) and Associate Prof. Motoo Utsumi (University of Tsukuba) for their appropriate advice and comments during the preparation of this dissertation.

Further, I wish to express my special gratitude to Prof. Teruyuki Nagamune (University of Tokyo) and Dr. Satoshi Yamaguchi (University of Tokyo) for giving me the opportunity to carry out this study and for offering various support, discussion and advice for my research. Also, I am indebted to Dr. Masao Murakawa (Asubio Pharma Co., Ltd.) for encouragement and helpful guidance in writing this thesis.

Finally, I would like to thank all of the individuals including my family who provided me with support and encouragement throughout my Ph.D study and life in general.

References

1. Teramura, Y.; Iwata, H. Cell surface modification with polymers for biomedical studies. *Soft Matter* **2010**, *6*, 1081–1091.
2. Schwarze S.R.; Hruska K.A., Dowdy S.F. Protein transduction: Unrestricted delivery into all cells? *Trends Cell Biol.* **2000**, *10*, 290–295.
3. Panza J.L.; Wangner W.R.; Rilo H.L.R.; Rao R.H.; Beckman E.J.; Russell A.J. Treatment of rat pancreatic islets with reactive PEG. *Biomaterials* **2000**, *21*, 1155–1164.
4. Saxon E.; Bertozzi C.R. Cell surface engineering by a modified Staudinger reaction. *Science* **2000**, *287*, 2007–2010.
5. Kato, K.; Itoh, C.; Yasukouchi, T.; Nagamune, T. Rapid protein anchoring into the membranes of mammalian cells using oleyl chain and poly(ethylene glycol) derivatives. *Biotechnol. Prog.* **2004**, *20*, 897–904.
6. Totani T.; Teramura Y.; Iwata H. Immobilization of urokinase on the islet surface by amphiphilic poly(vinyl alcohol) that carries alkyl side chains. *Biomaterials* **2008**, *29*, 2878–2883.
7. Rabuka D.; Forstner M.B.; Groves J.T.; Bertozzi C.R. Noncovalent cell surface engineering: incorporation of bioactive synthetic glycopolymers into cellular membranes. *J. Am. Chem. Soc*. **2008**, *130*, 5947–5953.
8. Chung, H.A.; Tajima, K.; Kato, K.; Matsummoto, N.; Yamamoto, K.; Nagamune, T. Modulating the actions of NK cell-mediated cytotoxicity using lipid-PEG (n) and inhibitory receptor-specific antagonistic peptide conjugates. *Biotechnol. Prog.* **2005**, *21*, 1226–1230.

9. Wang, T.; Leventis, R.; Silvius, J.R. Artificially lipid-anchored proteins can elicit clustering-induced intracellular signaling events in Jurkat T-lymphocytes independent of lipid raft association. *J. Biol. Chem.* **2005**, *280*, 22839–22846.

10. Teramura, Y.; Iwata, H. Surface modification of islets with PEG-lipid for improvement of graft survival in intraportal transplantation. *Transplantation* **2009**, *88*, 624–630.

11. Figdor, C.G.; de Vries, I.J.; Lesterhuis, W.J.; Melief C.J. Dendritic cell immunotherapy: mapping the way. *Nat. Med.* **2004**, *10*, 475−480.

12. Lu, W.; Wu, X.; Lu, Y.; Guo, W.; Andrieu, J.M. Therapeutic dendritic-cell vaccine for simian AIDS. *Nat. Med.* **2003**, *9*, 27–32.

13. Banchereau, J; Palucka, A.K. Dendritic cells as therapeutic vaccines against cancer. *Nat. Rev. Immunol.* **2005**, *5*, 296–306.

14. Nestle, F.O.; Farkas, A.; Conrad, C. Dendritic-cell-based therapeutic vaccination against cancer. *Curr. Opin. Immunol.* **2005**, *17*, 163–169.

15. Janikashvili, N.; Larmonier, N.; Katsanis, E. Personal dendritic cell-based tumor immunotherapy. *Immunotherapy* **2010**, *2*, 57–68.

16. Schnurr, M.; Scholz, C.; Rothenfusser, S.; Galambos, P.; Dauer, M.; Röbe, J.; Endres, S.; Eigler, A. Apoptotic pancreatic tumor cells are superior to cell lysates in promoting cross-priming of cytotoxic T cells and activate NK and γδ T cells. *Cancer Res.* **2002**, *62*, 2347–2352.

17. Akiyama, K.; Ebihara, S.; Yada, A.; Matsumura, K.; Aiba, S.; Nukiwa, T.; Takai, T. Targeting apoptotic tumor cells to FcγR provides efficient and versatile vaccination against tumors by dendritic cells. *J. Immunol.* **2003**, *170*, 1641–1648.

18. Galea-Lauri, J.; Darling, D.; Mufti, G.; Harrison, P.; Farzaneh, F. Eliciting cytotoxic T lymphocytes against acute myeloid leukemia-derived antigens: evaluation of dendritic cell-leukemia cell hybrids and other antigen-loading strategies for dendritic cell-based vaccination. *Cancer Immunol. Immunot.* **2002**, *51*, 299–310.

19. Kotera, Y.; Shimizu, K.; Mulé, J.J. Comparative analysis of necrotic and apoptotic tumor cells as a source of antigen(s) in dendritic cell-based immunization. *Cancer Res.* **2001**, *61*, 8105–8109.

20. Fernandez, N.C.; Lozier, A.; Flament, C.; Ricciardi-Castagnoli, P.; Bellet, D.; Suter, M.; Perricaudt, M.; Tursz, T.; Maraskovsky, E.; Zitvogel, L. Dendritic cells directly trigger NK cell functions: cross-talk relevant in innate anti-tumor immune responses *in vivo*. *Nat. Med.* **1999**, *5*, 405–411.

21. Kim, K.D.; Choi, S.C.; Kim, A.; Choc, Y.K.; Choc, I.S.; Lim, J.S. Dendritic cell-tumor coculturing vaccine can induce antitumor immunity through both NK and CTL interaction. *Int. Immunopharmacol.* **2001**, *1*, 2117–2129.

22. Regnault, A.; Lankar, D.; Lacabanne, V.; Rodriguez, A.; Théry, C.; Rescigno, M.; Saito, T.; Verbeek, S.; Bonnerot, C.; Ricciardi-Castagnoli, P.; Amigorena, S. Fcγ receptor-mediated induction of dendritic cell maturation and major histocompatibility complex class I-restricted antigen presentation after immune complex internalization. *J. Exp. Med.* **1999**, *189*, 371–380.

23. Ravetch, J.V.; Bolland, S. IgG Fc receptors. *Annu. Rev. Immunol.* **2001**, *19*, 275–290.

24. Chan, A.C.; Carter, P.J. Therapeutic antibodies for autoimmunity and inflammation. *Nat. Rev. Immunol.* **2010**, *10*, 301–316.

25. Ashraf, S.Q.; Umana, P.; Mossner, E.; Ntouroupi, T.; Brunker, P.; Schmidt, C.; Wilding, J.L.; Mortensen, N.J.; Bodmer, W.F. Humanised IgG1 antibody variants targeting membrane-bound carcinoembryonic antigen by antibody-dependent cellular cytotoxicity and phagocytosis. *Br. J. Cancer.* **2009**, *101*, 1758–1768.

26. Chapman, A.P. PEGylated antibodies and antibody fragments for improved therapy: a review. *Adv. Drug Del. Rev.* **2002**, *54*, 531–545.

27. Kratz, F.; Müller, I.A.; Ryppa, C.; Warnecke, A. Prodrug strategies in anticancer chemotherapy. *ChemMedChem* **2008**, *3*, 20–53.

28. Kitamura, K.; Takahashi, T.; Yamaguchi, T.; Noguchi, A.; Noguchi, A.; Takashina, K.; Tsurumi, H.; Inagake, M.; Toyokuni, T.; Hakomori, S. Chemical engineering of the monoclonal antibody A7 by polyethylene glycol for targeting cancer chemotherapy. *Cancer Res.* **1991**, *51*, 4310–4315.

29. Takahashi, H.; Wilson, B.; Ozturk, M.; Motté, P.; Strauss, W.; Isselbacher, K.J.; Wands, J.R. *In vivo* localization of human colon adenocarcinoma by monoclonal antibody binding to a highly expressed cell surface antigen. *Cancer Res.* **1988**, *48*, 6573–6579.

30. Shinkawa, T.; Nakamura, K.; Yamane, N.; Shoji-Hosaka, E.; Kanda, Y.; Sakurada, M.; Uchida, K.; Anazawa, H.; Satoh, M.; Yamasaki, M.; Hanai, N.; Shitara, K. The absence of fucose but not the presence of galactose of bisecting *N*-acetylglucosamine of human IgG1 complex-type oligosaccharides shows the critical role of enhancing antibody-dependent cellular cytotoxicity. *J. Biol. Chem.* **2003**, *278*, 3466–3473.

31. Suzuki, T.; Kanbara, N.; Tomono, T.; Hayashi, N.; Shinohara, I. Physicochemical and biological properties of poly(ethylene glycol)-coupled immunoglobulin G. *Biochim. Biophys. Acta* **1984**, *788*, 248–255.

32. Koning, G.A.; Morselt, H.W.; Kamps, J.A.; Scherphof, G.L. Uptake and intracellular processing of PEG-liposomes and PEG-immunoliposomes by kupffer cells *in vitro*. *J. Liposome Res.* **2001**, *11,* 195–209.

33. Chikh, G.G.; Kong, S.; Bally, M.B.; Meunier, J.C.; Schutze-Redelmeier, M.P. Efficient delivery of Antennapedia homeodomain fused to CTL epitope with liposomes into dendritic cells results in the activation of CD8+ T cells. *J. Immunol.* **2001**, *167*, 6462–6470.

34. Kawamura, K.; Kadowaki, N.; Suzuki, R.; Udagawa, S.; Kasaoka, S.; Utoguchi, N.; Kitawaki, T.; Sugimoto, N.; Okada, N.; Maruyama, K.; Uchiyama, T. Dendritic cells that endocytosed antigen-containing IgG-liposomes elicit effective antitumor immunity. *J. Immunother.* **2006**, *29*, 165–174.

35. Annunziata, L.; Elisa, B.; Pietro, T. Mass spectrometry of advanced glycation end products. *Adv. Clin. Chem.* **2005**, *40*, 165–217.

36. Eberl, H.; Tittmann, P.; Glockshuber, R. Characterization of recombinant, membrane-attached full-length prion protein. *J. Biol. Chem*. **2004**, *279*, 25058–25065.

37. Breydo, L.; Sun, Y.; Makarava, N.; Lee, C.I.; Novitskaia, V.; Bocharova, O.; Kao, J.P.Y.; Baskakov, I.V. Nonpolar substitution at the c-terminus of the prion protein, a mimic of the glycosylphosphatidylinositol anchor, partially impairs amyloid fibril formation. *Biochemistry* **2007**, *46*, 852–861.

38. Antos, J.M.; Miller, G.M.; Grotenbreg, G.M.; Ploegh, H.L. Lipid modification of proteins through sortase-catalyzed transpeptidation. *J. Am. Chem. Soc.* **2008**, *130*, 16338–16343.

39. Abe, H.; Goto, M.; Kamiya, N. Protein lipidation catalyzed by microbial transglutaminase. *Chem. Eur. J.* **2011**, *17*, 14004–14008.

40. Tsukiji, S.; Nagamune, T. Sortase-mediated ligation: a gift from gram-positive bacteria to protein engineering. *ChemBioChem* **2009**, *10*, 787–798.

41. Popp, M.W.; Ploegh, H.L. Making and breaking peptide bonds: protein engineering using sortase. *Angew. Chem. Int. Ed.* **2011**, *50*, 5024–5032.

42. Tanaka, T.; Yamamoto, T.; Tsukiji, S.; Nagamune, T. Site-specific protein modification on living cells catalyzed by Sortase. *ChemBioChem* **2008**, *9*, 802–807.

43. Nimmerjahn, F.; Ravetch, J.V. Fcγ receptors as regulators of immune responses. *Nat. Rev.* **2008**, *8*, 34–47.

44. García-García, E.; Rosales, C. Signal transduction during Fc receptor-mediated phagocytosis. *J. Leukoc. Biol*. **2002**, *72*, 1092–1108.

45. Guo, X.; Wu, Z.; Guo, Z. New method for site-specific modification of liposomes with protein using sortase A-mediated transpeptidation. *Bioconjug. Chem.* **2012**, *23*, 650–655.

46. Dozier, J.K.; Distefano, M.D. Site-specific PEGylation of therapeutic proteins. *Int. J. Mol. Sci.* **2015**, *16*, 25831–25864.